



# Polymeric composite materials for radiation shielding: a review

Chaitali V. More<sup>1</sup> · Zainab Alsayed<sup>2</sup> · Mohamed. S. Badawi<sup>2</sup> · Abouzeid. A. Thabet<sup>3</sup> · Pravina P. Pawar<sup>1</sup>

Received: 24 October 2020 / Accepted: 19 January 2021 / Published online: 3 February 2021  
© The Author(s), under exclusive licence to Springer Nature Switzerland AG part of Springer Nature 2021

## Abstract

The rising use of radioactive elements is increasing radioactive pollution and calling for advanced materials to protect individuals. For instance, polymers are promising due to their mechanical, electrical, thermal, and multifunctional properties. Moreover, composites made of polymers and high atomic number fillers should allow to obtain material with low-weight, good flexibility, and good processability. Here we review the synthesis of polymer materials for radiation protection, with focus on the role of the nanofillers. We discuss the effectiveness of polymeric materials for the absorption of fast neutrons. We also present the recycling of polymers into composites.

**Keywords** Ionizing radiation · Gamma radiation · Polymer composite materials · Polymer recycling and radiation shielding

## Abbreviations

$\gamma$ -rays	Gamma rays	WO <sub>3</sub>	Tungsten trioxide
Z	Atomic number	EPVC	Emulsion polyvinyl chloride
Bq	Becquerel	PolyBiz	Polymer bricks
C	Carbon	$\rho$	Density
H	Hydrogen	$M$	Mass
O	Oxygen	$V$	Volume
N	Nitrogen	$I_0$	Un-attenuated photon intensity
Ba	Barium	$I$	Attenuated photon intensity
Pb	Lead	$\mu_m$ or $\mu/\rho$	Mass attenuation coefficient
Al	Aluminium	$W_i$	Weight fraction
Cu	Copper	$A_i$	Atomic weight of <i>i</i> th element
Fe	Iron	$a_i$	Number of formula units
Bi	Bismuth	$Z_{\text{eff}}$	Effective atomic number
Bi <sub>2</sub> O <sub>3</sub>	Bismuth oxide	$\sigma_{\text{atm}}$ or $\sigma_a$	Total atomic cross-section
W	Tungsten	$\sigma_e$ or $\sigma_{\text{el}}$	Electronic cross-section
MoS <sub>2</sub>	Molybdenum disulfide	$\sigma_t$ or $\sigma_{\text{tot}}$	Total cross-section
B <sub>4</sub> C	Boron carbide	$\sigma_m$ or $\sigma_{\text{mol}}$	Total cross-section
PE	Polyethylene	$f_i$	Fractional abundance of <i>i</i> th constituent element
HDPE	High density polyethylene	$N_e$ or $N_{\text{eff}}$	Effective electron density
		$\langle A \rangle$	Average atomic mass of the material

✉ Chaitali V. More  
chaitalimore89@gmail.com

- <sup>1</sup> Department of Physics, Dr. Babasaheb Ambedkar Marathwada University, Aurangabad, MS, India
- <sup>2</sup> Department of Physics, Faculty of Science, Beirut Arab University, Beirut, Lebanon
- <sup>3</sup> Department of Medical Equipment Technology, Faculty of Allied Medical Sciences, Pharos University in Alexandria, Alexandria, Egypt

$\Lambda$  or MFP  
 $\mu$   
 $\epsilon$   
 $Z_{\text{eq}}$   
EABF  
EBF

Relaxation length  
Linear attenuation coefficient  
Molar extinction coefficient  
Equivalent atomic number  
Energy absorption build-up factor  
Exposure build-up factor

$\Sigma_R$	Macroscopic removal cross-section for fast neutrons	$Pb_3O_4$	Lead tetraoxide
HVT	Half value layer	$WO_3$	Tungsten oxide
TVL	Tenth value layer	$ZrO_2$	Zirconium dioxide
RPE	Radiation protection efficiency	UHMWPE	Ultra-high-molecular-weight polyethylene
G-P fitting method	Geometric-progression fitting method	P(VDF-TrFE)	Poly(vinylidene fluoride—trifluoroethylene)
POM	Polyoxymethylene	EVA	Ethylene vinyl acetate copolymer
PAN	Polyacrylonitrile	CB	Carbon black
NR	Natural rubber	W	Tungsten
PMA	Polymethyl acrylate	HSC	Hematite-serpentine concrete
PPM	Poly-phenyl-methacrylate	CdO	Cadmium oxide
PET	Polyethylene terephthalate	Pd/Ag alloy	Palladium/silver alloy
(PA-6)	Polyamide (Nylon 6)	PVA-PEG-PVP-ZrO <sub>2</sub>	Polyvinyl alcohol-polyethylene glycol-polyvinyl pyrrolidinone with zirconium oxide
PAN	Polyacrylonitrile		
PVDC	Polyvinylidene chloride		
PANI	Polyaniline	VMQ	Methyl vinyl silicone rubber
PET	Polyethylene terephthalate	Al <sub>2</sub> O <sub>3</sub>	Aluminium oxide
PPS	Polyphenylene sulfide	PDMS	Polydimethylsiloxane
PPy	Polypyrrole	WC	Tungsten carbide
PTFE	Polytetrafluoroethylene	W-BN	Tungsten-boron nitride
PVC	Polyvinyl chloride	EVA	Ethylene-vinyl acetate
PMMA	Polymethyl methacrylate	CMT	Colemanite
DMSO	Dimethyl sulfoxide	CMW	Coal mining waste
PEI	Polyethylenimine	CaCO <sub>3</sub>	Calcium carbonate
PVA	Poly(vinyl alcohol)	CFRTPCs	Carbon fiber reinforced thermoplastic composites
MCNP code	Monte Carlo N-particle code		
NaI (TI)	Thallium doped sodium iodide	COD	Chemical oxygen demand
SGS	Sol-gel synthesis	SPR	Smoke production rate
NPs	Nano particles	THR	Total heat release
IMS	Intermatrix synthesis	TPU	Thermoplastic polyurethane
SBR	Styrene-butadiene rubber	LBS	Lead-bearing sludge
Fe <sub>2</sub> O <sub>3</sub>	Ferric oxide	ABS	Poly(acrylonitrile-butadiene-styrene)
ZnO	Zinc oxide		
MoO	Molybdenum oxide	WrPC	Recycled plastic composite
TiO <sub>2</sub>	Titanium dioxide	UPR	Unsaturated polyester resin
ABS	Acrylonitrile butadiene styrene	Pb(NO <sub>3</sub> ) <sub>2</sub>	Lead nitrate
PLA	Polylactic acid	CeO <sub>2</sub>	Cerium dioxide
3D	3 Dimensional	Cs	Cesium
PC	Polycarbonate	Am	Americium
wt%	Weight percent	I	Iodine
PEEK	Poly-ether-ether-ketone	Co	Cobalt
IMS	Intermatrix synthesis	Gy	Gray
BNP	Bismuth nitrate pentahydrate	MCM	Mobil composition of matter
Gd <sub>2</sub> O <sub>3</sub>	Gadolinium oxide		
PVDF	Polyvinylidene difluoride		
BaTiO <sub>3</sub>	Barium titanate		
CaWO <sub>4</sub>	Calcium tungsten oxide		
LDPE	Low-density polyethylene		
PS	Polystyrene		
PP	Polypropylene		
PVP	Polyvinyl pyrrolidone		
PbO	Lead oxide		

## Introduction

Radiation is energy that comes from a source and travels through space and may be able to penetrate various materials. Radiation can be classified according to its capability to ionize matter into two main categories: (1) ionizing radiation and (2) nonionizing radiation (Singh et al. 2014a,

b). Nonionizing radiation does not possess enough energy to eject electrons from the atom and produce ions such as visible light, microwaves, radio waves, alpha, beta particles from radioactive substances, or neutrons from nuclear reactors, infrared, and sunlight (Oto et al. 2015). Ionizing radiation is electromagnetic radiation that carries higher energy than nonionizing radiation that makes them capable of ejecting electrons from atoms and produces negatively charged free electrons and positively charged ionized atoms. Ionizing radiation consists of any types of photons (X-rays and gamma ( $\gamma$ )-rays) or particles (alpha, beta, and neutrons) (Harish et al. 2012).

The use of high-energy ionizing radiations especially gamma rays is rapidly growing in many sectors like industries, nuclear reactors, medical diagnostics, nuclear research establishment, food irradiation, nuclear waste storage sites, biological studies, defects detecting in metal castings nuclear medical imaging, and therapy, space exploration, and high-energy physics experiments, and so on (Sayyed et al. 2017a, b). Inadvertent exposure to gamma rays which possess a highly energetic and penetrating nature is of great concern due to its detrimental effects on human life, the environment, and other materials. Further, for humans, this can engender radiation sickness, organ damage, cell mutation, cancer, component failure, and other harmful effects (Sayyed et al. 2019). Therefore, protection from the inimical effects of radiation for the human population and the environment is very important and it depends on four important factors: time, distance, shielding, and activity. By minimizing exposure time and increasing the distance, the dose from the source of radiation can be reduced. Since the distance from the source follows inverse square law which means that if the distance is doubled, then the dose/dose rate at the new location will quarter (Woodhead 2002). The activity, measured in Becquerel (Bq), is defined as the strength of a radioactive source which represents the number of atoms that decay and emit radiation in one second. Radioactive substances of different activities contain different hazards and thus must be handled accordingly (Choppin et al. 2002). Shielding is generally preferred for radiation protection. Shielding has merits such as it has independent efficacy in safe working conditions over the time of exposure and distance that require continued managerial regulation (Vahabi et al. 2017). Thus, an appropriate shielding against nuclear radiation is constantly in demand for a secure life and a healthy environment as the radiation uses are consistently viable in various human activities (Kumar 2017).

Researchers have investigated various radiation shielding materials to protect life and its surroundings from debasing consequences that occurred from radiation exposure under attenuation or absorption of unwanted radiations (Singh et al. 2014a, b; Al-Buriahi et al. 2020; Levet et al. 2020; More et al. 2020a, b; Rani et al. 2020). Weight, space, cost,

and attenuation or absorption capabilities of the materials used for radiological protection are key points that defy researchers to synthesize and develop appropriate shielding materials. A good radiation shield is one that can attenuate, absorb, or block the maximum part of incident gamma radiation. The nature and mechanism of interaction between gamma rays and materials is a critical issue to study to determine the ability of these radiations to diffuse and crack in the medium that according to the mechanism of interaction helps to choose the more applicable radiation shield. Materials that are supposed to be used as shields against gamma photons should have higher atomic number and density as such materials impose a higher probability of interactions that implies larger energy transfer with gamma rays (Chang et al. 2015). Withal, materials with lower atomic number (lower-Z) and density can make up of increased thickness as significantly as high atomic number (high-Z) materials in radiation protection (Luković et al. 2015; Mostafa et al. 2017). Customarily, lead, multiple layers of single slabs of pure elements such as barium (Ba), lead (Pb), aluminum (Al), copper (Cu), iron (Fe), and concrete are reliable efficient materials that prevent humans from getting affected by the obnoxious effects of ionizing radiations (Sayyed et al. 2017a, b). Despite having great radiation attenuation properties, lead and concrete are discarded due to the heterogeneous nature of lead, and moisture variation in concretes makes it hard to predict radiation protection (Singh et al. 2015) and insidious hazards are proposed by lead to human health and the environment (Thuyavan et al. 2015). In contrast to the past, polymer and its composites offer promising suitable alternative candidates to lead and concrete in the field of radiation shielding due to its lightweight, durability, flexibility along with superior physical, mechanical, optical, and radiation resistance properties (Ambika et al. 2017; Alavian et al. 2020). Besides, polymers can easily be doped with sizeable amounts of high atomic number (high-Z) materials to form their composites that are more competent radiation shields (Atashi et al. 2018).

Latterly, investigators working in the field of radiation protection have focused and reported numerous polymer matrices that can be used as gamma-ray shields like bismuth oxide ( $\text{Bi}_2\text{O}_3$ ) filled poly (methyl methacrylate) composites; high-density polyethylene (HDPE) composite loaded with tungsten (W), molybdenum sulfide ( $\text{MoS}_2$ ), and boron carbide ( $\text{B}_4\text{C}$ ); micro- and nanosized tungsten oxide ( $\text{WO}_3$ ) dispersed emulsion polyvinyl chloride (EPVC) polymer composites; lead oxide filled isophthalic resin polymer composites; silicone rubber composites containing bismuth content; polymer bricks (PolyBiz); polyester composites reinforced with zinc; composites of high-density polyethylene with zinc oxide; lead oxide; and cadmium oxide (Plionis et al. 2009; El-Fiki et al. 2015; Aghaz et al. 2016; Mahmoud

et al. 2018a, b; Afshar et al. 2019; Alsayed et al. 2019, 2020; El-Khatib et al. 2019; Cao et al. 2020; Kaçal et al. 2020).

The incorporation of a filler in a microsize range within the composite material leads to the enhancement of composite properties. Chemical and intermolecular forces render the bond between the polymer and the matrix. But on the nanometer scale, a nanofiller can be dispersed within the polymer matrix. Thus, the molecular interactions between the matrix and the filler are improved via chemical bonding leading to further enhancement in the mechanical and physical properties of the new polymer nanocomposites (Kumar et al. 2009). Nanofillers are characterized by a high surface-to-volume ratio which affects the alteration in the macromolecular state around the nanoparticles. The addition of nanofiller enhances the characteristics of the polymer such as increased elastic stiffness and strength, heat and barrier resistance, decreased gas permeability, and flammability. The optical, magnetic, electrical, and dielectric properties are also enhanced (Phong et al. 2013; Kumar et al. 2014). Another aspect that signifies the use of nanoparticles as additives to the polymer matrix is that the loading requirements are quite low compared to others. Various types of inorganic nanomaterials such as zeolite, zinc oxide, titanium oxide, and silicon dioxide were used with nanoclay materials to manufacture nanocomposite membrane which is effective in removing salts and minerals from seawater by process called desalination (Hebbar et al. 2017). Moreover, intensive recent studies focus on the evidence of low toxicity of mostly used nanoparticles such as copper, silver, and titania nanoparticles which were found to be having low toxicity in various natural media when subjected to oxic/anoxic suspension, and incubation with natural organic matter (Mulenos George et al. 2020).

Generally, polymers have very low mechanical characteristics but are useful because of their flexibility in applications requiring such a property. They are usually deformed at high strain under loading. The improvement in mechanical properties such as tensile strength, modulus, or stiffness is done by adding inorganic particles via reinforcement mechanisms. Such properties can indeed be tailored by changing the volume fraction, shape, and size of the filler particles. The better enhancement in mechanical properties can be gained with the reinforcement of nanofillers having a very large aspect ratio and stiffness in a polymer matrix (Bhattacharya 2016). Polymer nanocomposites offer the promise of a new generation of lightweight hybrid materials with numerous possibilities for automotive, general, and industrial applications. It includes the potential for utilization as radiation shielding materials over traditional materials. The high kinetic energy of neutrons makes them capable of passing through most materials and interacts immediately with atoms of the target material. Neutrons are generally used for the production of nuclear energy in nuclear power plants and

workers there get exposed to neutrons. Besides them, aircraft personnel is prone to exposure to neutrons. Exposure to neutrons is considered critical due to the detrimental effects on the human body as they generate much denser ion paths while they deposited their energy (Mirji and Lobo 2017a, b). Thus, there is a demand for efficient, durable, lightweight, and cost-effective materials to get protected from different types of radiation.

Since polymer composites are considered cornerstone's as engineering materials for many applications such as building, civil engineering, aerospace technology, electronics, and electrical engineering (Alavian and Tavakoli-Anbaran 2020). In addition, an important issue to be considered is the surface functionalization of polymer composites when nano-objects are added to ameliorate the performance of the synthesized material (Makvandi et al. 2020). An interesting problem arises from the use and storage of polymer composite materials as wastes. The accumulation of wastes from polymer composite materials can lead to a serious burden on humans and the environment by causing pollution to nature.

Recently, many researchers dedicated their efforts to develop new technologies for recycling and treatment of polymer composite materials waste (Turner et al. 2011). Recycling and incorporation of different filler materials in recycled polymers which can be easily composted (Adeosun et al. 2012) are extremely important to provide environmentally friendly and sustainable materials (Okamoto 2003). Many attempts have been dedicated to using biodegradable fillers which at the same time can enhance the performance of the composite (Lee et al. 2008; Qu et al. 2010). Other researchers were concerned about developing thermoplastic composites with recyclable fibers to diminish the use of fillers without any harm to the environment and keeping it clean and healthy (Kaushik et al. 2010; Zadegan et al. 2011).

In this review, the leading edge of polymer and its composites especially with nanomaterials' as radiation-shielding materials are epitomized. In "Polymers properties and applications" section, the properties of polymer materials have been discussed. "Physical and radiation shielding properties" section gives information about physical and radiation shielding properties of polymer materials, whereas "Polymers used in radiological protection" gives an overview and historical perspective along with a brief literature review of the polymer materials. In Sect. 5, synthesis methods of polymer composites have been discussed. Also, the contemporaneous work on polymer materials and the development of polymer composites as promising candidates for radiation shielding is broadly categorized and a brief literature review is presented. Improvement in the shielding abilities of polymers by the incorporation of nanofillers is presented in Sect. 6. In Sects. 7 and 8, recycling of polymers and the use of processed and post-consumed polymers as composite materials for different applications were covered,

respectively. In Sect. 9, the use of polymeric materials for neutron shielding has been covered. The comparative study of polymer composites is given in Sect. 10. Conclusions and future aspects have been outlined in Sects. 11 and 12, respectively.

### Polymers properties and applications

Polymers are substances containing a large number of structural units joined by the same type of linkage. These substances often form a chain-like structure. It has been approximately 60 years since researchers first began exposing polymeric materials to ionizing radiations, and today, a substantial commercial industry is in place based on the processing of polymers with radiation. Polymers are of low atomic number and low density and thus lightweight materials. Polymers possess high durability, and they are tough. Also, they are cost-effective, need low maintenance, and stable over a wide temperature range (Alavian and Tavakoli-Anbaran 2019). Based on processing under changing temperature, polymers are categorized as thermosets and thermoplastics as listed in Fig. 1, also thermoplastics including elastomers can be divided into semicrystalline and amorphous polymers. Both the thermoset and thermoplastic

polymers have some pros and cons, but thermoplastics are preferred for radiation shielding applications due to their superior properties as shown in Table 1. Also, thermoplastic polymers are highly recyclable and possess remolding abilities and eco-friendly manufacturing is possible using them (Cassagnau et al. 2007).

Polymers proved their effectiveness in wide range of applications including CO<sub>2</sub> capture (Chatterjee and Krupadam 2018), safe gene delivery (Daima et al. 2018), dye removal (Grégorio et al. 2019), water and wastewater treatment (Lichtfouse et al. 2019), metal ions removal from wastewater (Salipira et al. 2007; Gu et al. 2018; Mao et al. 2018), and drug delivery (Parhi 2020).

### Physical and radiation shielding properties

#### Density

“Density ( $\rho$ ) is a measure of mass ( $M$ ) per unit volume ( $V$ ) of a substance.” Its unit is  $\text{g/cm}^3$ . Density is an important physical characteristic of a material that helps to decide the radiation shielding ability of a material. It is well known that the higher the density of the material, the higher will be the

**Fig. 1** Polymers are categorized as thermosets and thermoplastics under changing temperature which can be divided into semicrystalline and amorphous

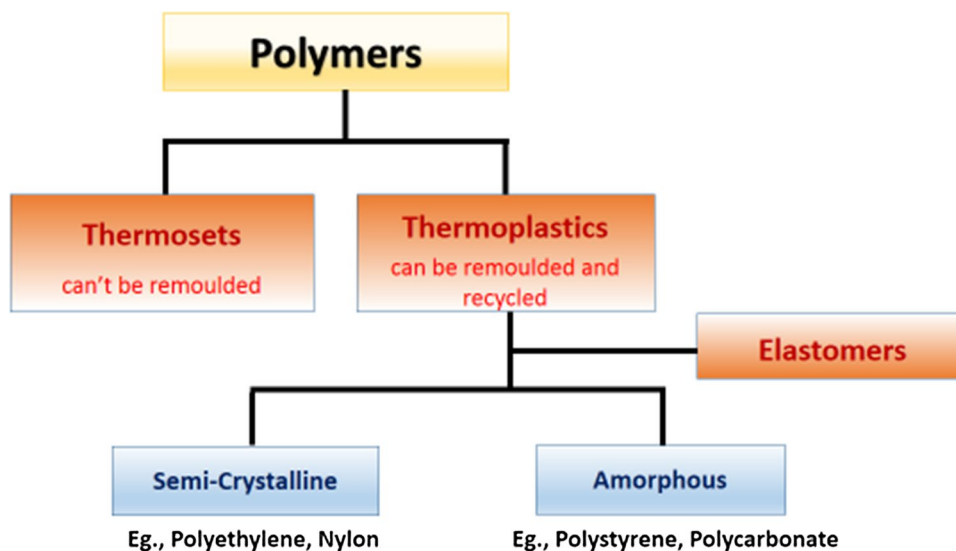


**Table 1** Comparison of properties of thermoset and thermoplastic polymers (Liu and Piggott 1995; Njuguna et al. 2007)

Polymer type	Toughness	User temperature	Processing time	Solvent resistance	Shear strength
Thermoplastic	High	Low	Low	Low	High
Toughened thermoset	↑Kaçal et al. (2019)	↓	↓	↓	↑
Lightly cross-linked thermoplastic					
Thermoplastic	Low	High	High	High	Low

chance of the probability of interaction between the incident photon and absorbing material (Hellström et al. 2017).

$$\rho = \frac{M}{V} \quad (1)$$

## Hardness

Hardness also known as structural strength is an important characteristic of the material that states the maximum load that the material can bear. There are several methods for calculating the hardness of a material such as young's modulus of rigidity, Rockwell hardness test, and Vickers microhardness tester. The hardness of the material makes it able to resist plastic deformation, penetration, and scratching (Chandler 1999).

## Linear and mass attenuation coefficients

A parallel beam of mono-energetic gamma-ray photons is attenuated in the matter according to the Lambert–Beer law,

$$I = I_0 e^{-\left(\frac{\mu}{\rho} \times \rho t\right)} \quad (2)$$

where  $I_0$  and  $I$  are the un-attenuated and attenuated photon intensities respectively,  $t$  (cm) is the sample thickness,  $\mu$  ( $\text{cm}^{-1}$ ) is the linear attenuation coefficient, and  $\rho$  ( $\text{g}/\text{cm}^3$ ) is a measured density of the sample (More et al. 2016).

The mass attenuation coefficient ( $\mu/\rho$ ) for any chemical compound or mixture of elements is given by

$$\left(\frac{\mu}{\rho}\right)_c = \sum_i w_i \frac{\mu}{\rho} \quad (3)$$

where  $w_i$  is the weight fraction and  $(\mu/\rho)_i$  is the mass attenuation coefficient of the  $i$ th constituent element. For a chemical compound, the weight fraction is given by

$$w_i = \frac{a_i A_i}{\sum_j a_j A_j} \quad (4)$$

where  $A_i$  is the atomic weight of  $i$ th element and  $a_i$  is the number of formula units. Figure 2 represents the schematic view of the narrow beam good geometry setup including a radioactive point source which is set based on a specific measurements, the sample, the detector, a high-voltage source (HV), an amplifier (Amp), and a multi-channel analyzer (MCA) which are all connected to a dedicated computer software.

## Effective atomic and electron number

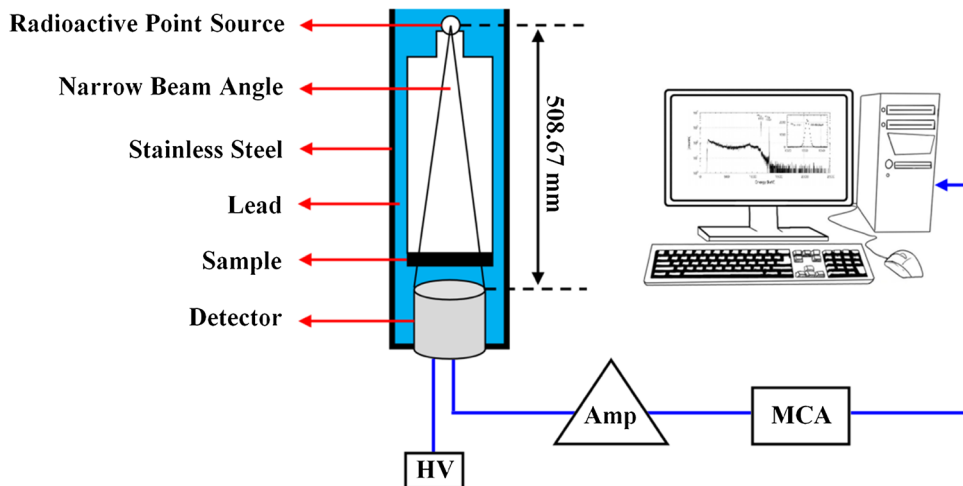
An effective atomic number ( $Z_{\text{eff}}$ ) is an important parameter for the determination of a substitute material for an element associated with the required energy. It fluctuates with energy, resembles the atomic number of elements, and describes the material's composition based on equivalent elements. The effective atomic number is obtained by the following equation (More et al. 2016)

$$Z_{\text{eff}} = \frac{\sigma_a}{\sigma_e} \quad (5)$$

Here,  $\sigma_a$  and  $\sigma_e$  are total atomic cross section and electronic cross section, respectively, and are given as follows (Sayed et al. 2017a, b):

$$\sigma_a = \frac{\mu_m}{N_A \sum_i \frac{w_i}{A_i}} \quad (6)$$

**Fig. 2** Narrow beam good geometry setup including a radioactive point source which is set based on a specific measurements, the sample, the detector, a high-voltage source (HV), an amplifier (Amp), and a multichannel analyser (MCA) which are all connected to a dedicated computer software (Sayed et al. 2020)



$$\sigma_e = \frac{1}{N_A} \sum_i \frac{f_i A_i}{Z_i} (\mu_m)_i \quad (7)$$

where  $f_i$  is the fractional abundance of  $i$ th constituent element and it can be given as the following:

$$f_i = \frac{n_i}{\sum_i n_i} \quad (8)$$

Effective electron density ( $N_{\text{eff}}$ ) is related to the effective atomic number and is given in the number of electrons per unit mass by the next equation (Azadbakht and Bagheri 2019):

$$N_{\text{eff}} = \frac{N_A}{\langle A \rangle} Z_{\text{eff}} \quad (9)$$

where  $\langle A \rangle$  is the average atomic mass of the material.

### Relaxation length

The average distance between two successive interactions is called the relaxation length. It is also called as photon mean free path ( $\lambda$ ). It can be calculated using the value of the linear attenuation coefficient,  $\mu$  ( $\text{cm}^{-1}$ ) (Akkurt and El-Khayatt 2013).

$$\lambda = \frac{1}{\mu} \quad (10)$$

### Half-value layer and tenth value layer

Half-value layer (HVL) and tenth value layer (TVL) are defined as the thickness or layer of a shield or absorber that lessens the intensity of radiation by a factor of one half and one tenth of the initial intensity, respectively (Mann et al. 2016).

$$\text{HVL} = \frac{\ln 2}{\mu} \quad (11)$$

$$\text{TVL} = \frac{\ln 10}{\mu} \quad (12)$$

### Radiation protection efficiency

The radiation protection efficiency of a material is an important parameter to know material's shielding ability and is determined as follows (Harima 1983):

$$\text{RPE} = \left( 1 - \frac{I}{I_0} \right) \times 100 \quad (13)$$

### Buildup factor

There are several reported methods for the calculation of buildup factors (Taylor 1954; Suteau and Chiron 2005; Vahabi and Shamsaie Zafarghandi 2020). The computation of energy absorption and exposure buildup factors (EABF and EBF) using widely used G-P fitting method and equivalent atomic number for selected Polymers is given step by step as follows:

### Calculation of equivalent atomic number ( $Z_{\text{eq}}$ )

The equivalent atomic number,  $Z_{\text{eq}}$ , depends on the chemical composition of materials. The obtained values of Compton partial mass attenuation coefficient,  $(\mu/\rho)_{\text{Comp}}$ , and the total mass attenuation coefficient,  $(\mu/\rho)_{\text{total}}$ , values for the elements  $Z=4-30$ , and for the selected materials using the XCOM/WinXCom program (Berger and Spencer 1959; Berger and Hubbell 1987; Gerward et al. 2004). The equivalent atomic number, for a given material, is then determined by matching the ratio,  $(\mu/\rho)_{\text{Comp}}/(\mu/\rho)_{\text{total}}$ , of that material at given energy with the corresponding ratio of a pure element at the same energy. If this ratio lies between the two ratios for known elements, then the value of  $Z_{\text{eq}}$  is interpolated using the following formula (Singh et al. 2014a, b):

$$Z_{\text{eq}} = \frac{Z_1(\log R_2 - \log R) + Z_2(\log R - \log R_1)}{(\log R_2 - \log R_1)} \quad (14)$$

where  $Z_1$  and  $Z_2$  are the atomic numbers of elements corresponding to the  $(\mu/\rho)_{\text{Comp}}/(\mu/\rho)_{\text{total}}$  ratios,  $R_1$  and  $R_2$ , respectively, and  $R$  is the corresponding ratio for a given polymer at given energy that lies between  $R_1$  and  $R_2$ .

### Estimation of geometric progression (G-P) parameters

Utilizing buildup factor data provided by American National Standards (ANSI/ANS 1991), geometric progression (G.P.) fitting parameters ( $b$ ,  $c$ ,  $a$ ,  $X_k$ , and  $d$ ) for selected polymer material in the energy range of 0.015–15 meV up to penetration depth of 40 mean free path (mfp) is computed with the help of equivalent atomic number ( $Z_{\text{eq}}$ ) using interpolation formula. Interpolation values were obtained with the use of the following equation:

$$P = \frac{P_1(\log Z_2 - \log Z_{\text{eq}}) + CP_2(\log Z_{\text{eq}} - \log Z_1)}{(\log Z_2 - \log Z_1)} \quad (15)$$

where  $P_1$  and  $P_2$  are the values of the coefficients of G-P fitting parameters corresponding to the atomic numbers  $Z_1$  and  $Z_2$ , respectively, at given energy and  $Z_{\text{eq}}$  is the equivalent atomic number of the selected material.  $Z_1$  and  $Z_2$  are the elemental atomic numbers between which the equivalent atomic number  $Z$  of the chosen samples lies.

### Calculation of energy absorption and exposure buildup factor

The energy absorption and exposure buildup factors for the selected samples for incident photon energies (0.015–15 meV) up to a penetration depth of 40 mean free paths have been calculated using estimated five geometric progression (G.P.) fitting parameter which is given below (Singh et al. 2014a, b):

$$B(E, X) = 1 + \frac{b-1}{K-1}(K^x - 1) \quad \text{at } K \neq 1 \quad (16)$$

$$B(E, X) = 1 + (b-1) \quad \text{at } K = 1 \quad (17)$$

$$K(E, x) = cx^a + d \frac{\tanh\left(\frac{x}{X_k} - 2\right) - \tanh(-2)}{1 - \tanh(-2)} \quad x \leq 40 \text{ mfp}$$

where  $E$  is the source energy and  $x$  is the penetration depth in the units of mean free path (mfp). Parameters  $b$  and  $K$  are corresponding to a buildup factor at 1 mean free path and a multiplication factor of dose through 1 mean free path (mfp) photon penetration, respectively, and  $a$ ,  $b$ ,  $c$ ,  $d$ , and  $X_k$  are geometric progression (G.P.) fitting parameters.

## Polymers used in radiological protection

### Overview and historical perspective

Many types of materials have been used as radiation shielding barriers to keep a safe environment for everyday practice in all radiation facilities. Many features can categorize the proper shielding material to be used including a high atomic number (high- $Z$ ) for gamma radiation shieldings such as barium (Ba), lead (Pb), and bismuth (Bi) (Kaçal et al. 2021), whereas elements of low atomic numbers are preferably used for neutron attenuation. However, many constraints burden the use of such traditional shielding materials such as the cost, heaviness, and toxicity.

The urgent need for alternative materials in radiation shielding stimulated synthesis, and manufacturing of polymeric and plastic materials, which became a cornerstone in the materials science industry. Polymers in the form

of bonded molecules (Callister 2007) are proposed in the radiation shielding industry due to their significant properties such as elasticity, compatibility, low cost, and lightness which nominate them as good candidates for radiation attenuation. Furthermore, polymers are materials containing elements with a low atomic number such as carbon (C), hydrogen (H), oxygen (O), and nitrogen (N) which are extremely important in medical applications used as tissue equivalent and phantom materials that resemble the human body. Polymers are frequently used in everyday life such as industrial (Kaphle et al. 2017), research, tissue engineering (Song et al. 2018), electronics, and drug delivery (Alavian and Tavakoli-Anbaran 2020). So the interaction of polymer material with radiation determines their contribution to the fields of science and applications. Usually, materials having dense structures are better in radiation resistance due to a high degree of symmetry. The interaction between organic material and radiation is governed by many mechanisms such as oxidation, gas production, and depolymerization (Tsepelev et al. 2019; Wady et al. 2019). In polymers, radiation resistance depends on oxygen rate and volume present in the material. Organic polymer materials are characterized by lightweight, corrosion resistance, low dielectric constant, and lightness, which allow their application in many fields containing radiation hazard.

### Brief literature review

Many researchers reported the use of polymers and polymer-based materials in the field of radiation shielding. This concern has been growing towards using eco-friendly and lead-free materials since lead poses a great hazard to both human health and the environment.

The X-ray and gamma radiation shielding properties of silicon polymers such as polymer A-poly dimethyl siloxane ( $\text{C}_2\text{H}_6\text{OSi}$ ), polymer B-polymethyl hydro-siloxane ( $\text{CH}_4\text{SiO}$ ), polymer C-per hydro-polysiloxane ( $\text{H}_3\text{SiN}$ ), polymer D-poly dimethyl siloxane ( $\text{C}_2\text{H}_6\text{Si}$ ), polymer E-methylsiloxane quinoxaline ( $\text{C}_{12}\text{H}_{32}\text{O}_8\text{Si}_8$ ), and polymer F-silalkalyene polymer ( $\text{SiC}_3\text{H}_8$ ) were studied. So that polymethyl hydro-siloxane ( $\text{CH}_4\text{SiO}$ ) possessed the lowest values of half-value layer, tenth value layer and mean free path (HVL, TVL, and  $\lambda$ ), and the highest attenuation coefficient (Nagaraja et al. 2020). Another type of polymer blends was prepared via compression molding, where MCNP5 simulation geometry would be suitable to study the radiation shielding performance of polyamide 6/acrylonitrile butadiene styrene blends against gamma rays for various energies (Abdel-Haseiba et al. 2018). Using a spectrophotometric technique, the radiation effect of  $^{60}\text{Co}$  gamma rays on a polycarbonate detector was investigated and the obtained results indicated that the polycarbonate revealed good performance to be used as a gamma radiation dosimeter (Galante and Campos 2010).

Besides, polymers proved their performance and applicability in nuclear medicine as radiation shielding against Technetium-99m, where complexed grafted low-density polyethylene films revealed that the protection efficiency of complexed grafted films was higher than in grafted and virgin films (Awadallah-F and Antar 2014). Also, most frequently used polymers such as POM—polyoxymethylene, PAN—polyacrylonitrile, NR—natural rubber, PEA—polymethyl acrylate, PPM—poly-phenyl-methacrylate, PET—polyethylene terephthalate (Bhosale et al. 2017) and polyamide (nylon 6) (PA-6), polyacrylonitrile (PAN), polyvinylidene chloride (PVDC), polyaniline (PANI), polyethylene terephthalate (PET), polyphenylene sulfide (PPS), polypyrrole (PPy), and polytetrafluoroethylene (PTFE) (Kaçal et al. 2019) were studied in terms of their gamma radiation attenuation. Polyacrylonitrile, natural rubber, and polyvinylidene chloride have the highest attenuation coefficient values. Furthermore, there is a remarkable increase in attenuation especially in the high energy region for barite, marble, and limra (Akkurt et al. 2009) and also for polyvinyl chloride (PVC) among six polymer and plastic materials: bone-equivalent plastic (B-100), polyvinyl chloride (PVC), air-equivalent plastic (C-552), radio chromic dye film (nylon base), polyethylene terephthalate (mylar), polymethyl methacrylate (PMMA), and concrete (NBS) in the energy range 10–1400 keV. Polyvinylidene chloride (PVC) revealed the highest shielding performance against gamma rays (Mann et al. 2015a, b). Also, resin 250 WD revealed good performance in neutron shielding applications compared to K-resin, epoxy resin, and resin which were studied by Elmahroug et al. (2014) for gamma ( $\gamma$ ) ray and neutron absorption. Among the selected samples, resin 250 WD is a good material for neutrons shielding applications. Epoxy resin and resin showed slightly better gamma rays shielding abilities than those of the other resin for applications. Using Monte Carlo simulation code, bone-equivalent plastic, polyvinylidene chloride, air-equivalent plastic, radio chromic dye film, polyethylene terephthalate, and polymethyl methacrylate was investigated in terms of values of mass attenuation coefficient and half-value layer ( $\mu_m$  and HVL) showing that the nylon-based radio chromic dye film has better shielding effectiveness than concrete for energies above 100 keV (Gurler and Akar Tarim 2016). Applying MCNP simulation for low atomic number (low-Z) materials such as polypropylene, perspex, bakelite, teflon, polyethylene, poly-carbonate, nylon 6–6, and polymethyl methacrylate (PMMA) polymers in the energy range of 59.5–1332.5 keV revealed good agreement with experimental and XCOM values. Thus, the used simulation geometry in the reported work can be used as an alternative method for the experiments for MCNP simulation for low-Z materials (Singh et al. 2015). Also, dimethyl sulfoxide (DMSO) and polyethylenimine (PEI) polymers have been studied by (Sayed 2016)

for their possible application for  $\gamma$ -rays and neutron shielding. Mass attenuation coefficient ( $\mu/\rho$ ), effective atomic and electron number ( $Z_{\text{eff}}$  and  $N_e$ ) in the wide energy range of 1 keV–100 GeV along with macroscopic removal cross section for fast neutrons ( $\Sigma_R$ ) have been calculated. Dimethyl sulfoxide showed superior shielding properties than polyethylenimine for gamma ( $\gamma$ )-ray, whereas polyethylenimine is a good material for neutron absorption. Moreover, the interaction parameters linear and mass attenuation coefficient, mass energy absorption coefficients, kinetic energy released per unit mass, and equivalent atomic number ( $\mu$ ,  $\mu/\rho$ ,  $\mu_{\text{en}}/\rho$ , KERMA, and  $Z_{\text{eq}}$ ) of gamma rays for different materials in the wide energy range of 1 keV–100 GeV were studied for bone-equivalent plastic, air-equivalent plastic, radio chromic dye film, polyethylene terephthalate, polymethyl methacrylate (PMMA), and polyvinyl chloride (PVC) polymers. Polyvinyl chloride showed better shielding performance, and it is even superior to NBS concrete (Mann et al. 2016). Also, in the energy range, 300–2000 keV, polymers including polyethylene (PE), polystyrene, polycarbonate, poly(vinyl alcohol), polyvinyl chloride, polyethylene terephthalate, polyvinyl pyrrolidone, polytetrafluoroethylene, polypropylene, and polymethyl methacrylate showed values of mass attenuation coefficients in good agreement with NIST data 300–2000 keV for all studied polymers. These data would use in selecting good shielding material (Mirji and Lobo 2017a, b). Vahabi et al. (2017) have reported mass attenuation coefficients for determined using MCNP4C code and XCOM program for poly-propylene, perspex, bakelite, teflon, polyethylene, polycarbonate, nylon 6–6, and polymethyl methacrylate (PMMA). It was observed that simulated results fit well with XCOM values and experimental results in the energy range of 59.5–1332.5 keV. From the results, it can be concluded that the simulation geometry used here can be used as an alternative method for the experiments. FLUKA Monte Carlo code and XCOM program were used as an efficient alternative tool to determine radiological parameters mass attenuation coefficient, relaxation length, half and tenth value layer, electronic and atomic cross section, effective atomic number, and electron density ( $\mu_m$ ,  $\lambda$ , TVL, HVL,  $\sigma_{\text{t,el}}$ ,  $\sigma_{\text{t,a}}$ ,  $Z_{\text{eff}}$ , and  $N_{\text{el}}$ ) of the polymeric materials: polytetrafluoroethylene, bakelite, polyethylene terephthalate, polypropylene, polysulfone, polystyrene, polyethylene, natural rubber, polymethyl methacrylate, and polyvinylchloride (Sharma et al. 2019). Polymers that are best suited to gamma irradiation for manufacturing N95 masks were identified. The findings showed that having the lowest (tenth and half-value layer) TVL, HVL, and mean free path (MFP), the N2 sample [polyvinylchloride (PVC)] has the best radiation attenuation performance and is the most promising mask sample when it comes to gamma-ray attenuation features (Kilicoglu et al. 2021).

Mass attenuation coefficient ( $\mu_m$ ) and other derived parameters such as linear attenuation coefficient, atomic, total and electronic cross section, effective atomic number, electron density, half-value layer, and tenth value layer ( $\mu$ ,  $\sigma_a$ ,  $\sigma_t$ ,  $\sigma_e$ ,  $Z_{\text{eff}}$ ,  $N_{\text{el}}$ ,  $\lambda$ , HVL, and TVL) for few thermoplastic polymers with the help of NaI (TI) detector and WinXCom program revealed good agreement between experimental, theoretical, and simulated values of all parameters confirming the competency of the tested polymers in nuclear medicine gamma shielding (More et al. 2020a, b). Also, using the same experimental setup, few polymers have been studied with the determination of mass attenuation coefficient, total cross section, molar extinction coefficient, effective atomic number, and electron density ( $\mu_m$ ,  $\sigma_t$ ,  $\sigma_e$ ,  $\epsilon$ ,  $Z_{\text{eff}}$ , and  $N_{\text{eff}}$ ) for gamma-ray shielding application using NaI (TI) scintillation detector and XCOM program. Among the chosen samples, nylon 1,1 showed better shielding capabilities (More et al. 2017). Polymethyl methacrylate and kapton polyimide polymers were investigated and their gamma-ray attenuation parameters such as mass attenuation coefficient, total and electronic cross section, molar extinction coefficient, effective atomic number, and electron density were measured using NaI (TI) crystal detector in the energy range 84–1330 keV. Energy absorption and exposure buildup factors have also been calculated and reported for the selected polymers (Manjunatha 2017). For a locally developed polymeric material, namely poly-boron, mass attenuation coefficient values have been computed using the analytical method for shielding application. The calculated values were compared with values calculated based on the WinXCom program, and a good agreement has been observed between these two values. Also, linear attenuation coefficients and relaxation length have been determined. Linear and mass attenuation coefficient values for poly-boron were found to be greater than those for pure polyethylene and borated polyethylene (Biswas et al. 2016).

All these studies for pure polymers for their use in radiological protection are very useful. These studies have great significance to choose a better polymer material that would be used in radiation shielding. Once getting complete information about a better polymer material, it becomes easy to reinforce it for the needed application.

Furthermore, it can be noticed that researchers have to focus on thermoplastic materials such as polyetherimide, kapton, polysulfone, polypropylene, polyether ketone, polymethyl methacrylate, poly (butylene terephthalate), poly (ether sulfone), polymethyl pentane, poly (butyl methacrylate), poly (phenylene oxide), high-density polyethylene, poly (ethylene isophthalate) and these thermoplastic materials help in control plastic pollution as they can be recycled.

### Preparation methods for polymer composites

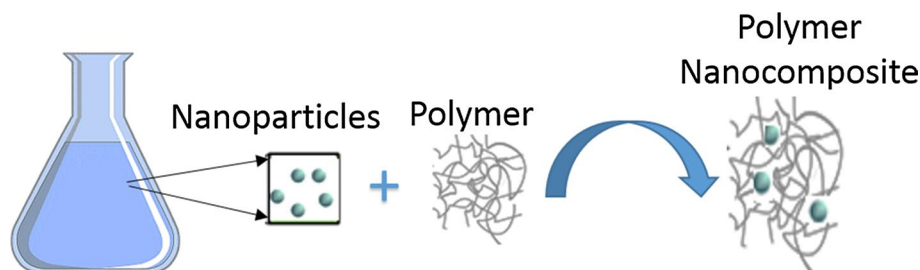
Several types of commercially available inorganic filler molecules can be incorporated in the polymer matrix to enhance their properties by the use of several synthesis methods. A few techniques for the fabrication of polymer composites are discussed below:

#### In situ synthesis

There are three types of in situ synthesis as follows: in situ polymerization, in situ synthesis of inorganic nanoparticles in a polymer matrix, and in situ intercalative polymerizations. In situ polymerization methods, the inorganic nanoparticles, are introduced to the monomer precursor for the desired polymer matrix in the liquid state, dispersed thoroughly, either in the presence or in the absence of a solvent, and then the monomer is polymerized with the nanofiller by adding the appropriate catalyst or initiators under certain conditions. Thermoplastic- and thermoset-based nanocomposites can be synthesized via this route.

Figure 3 reveals the in situ technique for polymer nanocomposites where nanoparticles are added to polymer matrix to form polymer nanocomposite. This method is significant and efficient for synthesizing composites starting from nanoparticles as precursors with the presence of polymer matrices. The first step in this process is explained by the nucleation of nanoparticles and their growth within the matrix of the polymer so that the aggregation of nanoparticles caused by handling and isolation is hindered. This technique represents a good advantage in terms of stabilization of the functional groups attributed to the polymer with the synthesized nanoparticles. Thus, particle size can be controlled and the

**Fig. 3** In situ synthesis for polymer nanocomposites where nanoparticles are added to polymer matrix to form polymer nanocomposite



agglomeration of nanoparticles is prevented as well as good spatial distribution is maintained (Ameen et al. 2012).

In situ intercalative polymerization is a highly efficient technique with a simple procedure based on the dispersion of the filler in the polymer precursors. It is usually utilized to prepare nanocomposites based on thermoset polymers. In a monomer solution, the fillers as nanoparticles are inflated to form intercalated sheets with the polymer matrix. There are two ways to initiate the polymerization: heat and radiation via diffusing an appropriate filler as an initiator or via cation exchange taking place after nanoparticle swelling. In situ intercalative polymerization technique possesses several advantages such as it is theoretically solvent-free and combines the polymerization and intercalation steps into a single, simultaneous process (Chen et al. 2009).

### In situ intercalative polymerization

In situ intercalative polymerization is a highly efficient technique with a simple procedure based on the dispersion of the filler in the polymer precursors. It is usually utilized to prepare nanocomposites based on thermoset polymers (Avella et al. 2001). In this technique, the nanofillers are swollen within the liquid monomer or a monomer solution so the polymer formation can take place between the intercalated sheets. Polymerization can be initiated either by heat or radiation, by the diffusion of a suitable initiator, or by an organic initiator or catalyst fixed through cation exchange inside the interlayer before the swelling step by the monomer. In situ intercalative polymerization technique possesses several advantages such as it is theoretically solvent-free and combines the polymerization and intercalation steps into a single, simultaneous process.

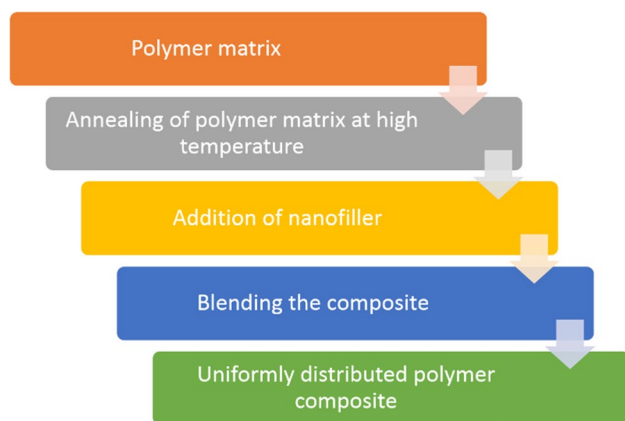


**Fig. 4** Melt intercalation method steps: preparing the polymer matrix which is followed by annealing at high temperature and then adding the nanofiller, and all the mixture is blended to form a uniformly distributed polymer composite

### Melt intercalation

Melt intercalation and hot pressing processes (also called melt blending method) are the typical standard approaches for synthesizing thermoplastic polymer nanocomposites. As shown by Fig. 4, it involves annealing the polymer matrix at high temperatures (above its softening point) statistically or under the shear, adding the nanofiller, and finally blending the composite to optimize the polymer–filler interactions and achieve uniform distribution. The melt intercalation technique has great advantages over either in situ intercalative polymerization of polymer solution intercalation. For example, melt intercalation is highly specific for the polymer, leading to new hybrids that were previously inaccessible. Besides, the lack of organic solvent usage makes melt intercalation an environmentally friendly and economically favorable method for industries from a waste perspective (Zeng et al. 2002).

### Sol-gel process

The sol-gel synthesis (SGS) illustrated in Fig. 5 is a process of solidifying a compound which contains a highly reactive component via sol-gel or solution which is followed by annealing and heat treatment. This process belongs to waste-free methods, and recently, it has been employed not only to prepare organic/inorganic composites but also to provide high-performance materials at lower temperatures and lower cost. The sol-gel route has been applied broadly because of its capability to control the miscibility between organic and inorganic components at the molecular level (Camargo et al. 2009). The major advantage of the sol-gel process is the high purity, high chemical homogeneity, and rigorous stoichiometry control associated with mild conditions, such as relatively low temperature and pressure.

### Ultrasound cavitation

The ultrasound cavitation technique is considered one of the most promising techniques for intensifying chemical/physical processing applications. Figure 6 summarizes the steps in the ultrasound cavitation technique; a solution containing a nanopolymer composite is prepared after mixing two solutions A and B, after that a sonicator probe is immersed, and using a pulse controller, ultrasound is applied. A sound wave consisting of successive compression (increase in local pressure) and rarefaction (decrease in local pressure) cycles is applied to a liquid. Then, the liquid starts oscillating tuned with the sound waves. Cavitation is mainly due to the generation, growth, and collapse of cavities which produce high energy densities at plenty of locations in a reactor simultaneously, thus resulting in very high conditions of pressure

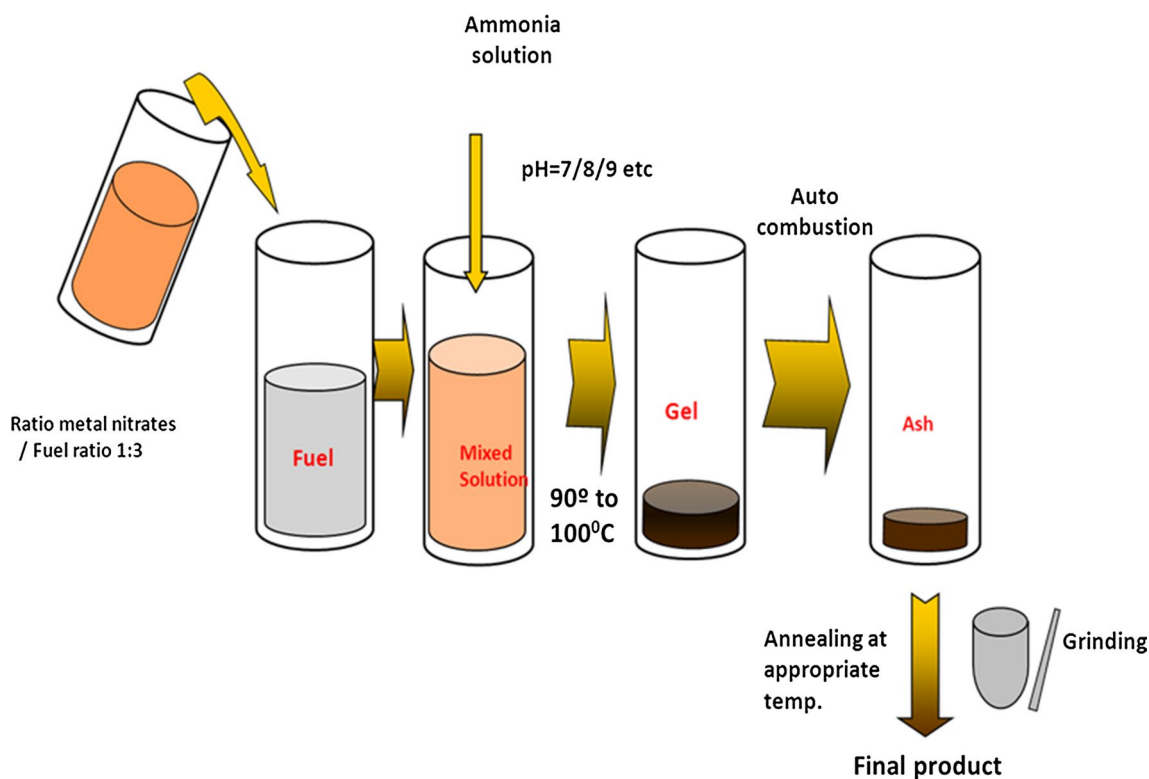


**Fig. 5** Sol-gel synthesis of where a compound which contains a highly reactive component is solidified via sol-gel or solution which is followed by annealing and heat treatment

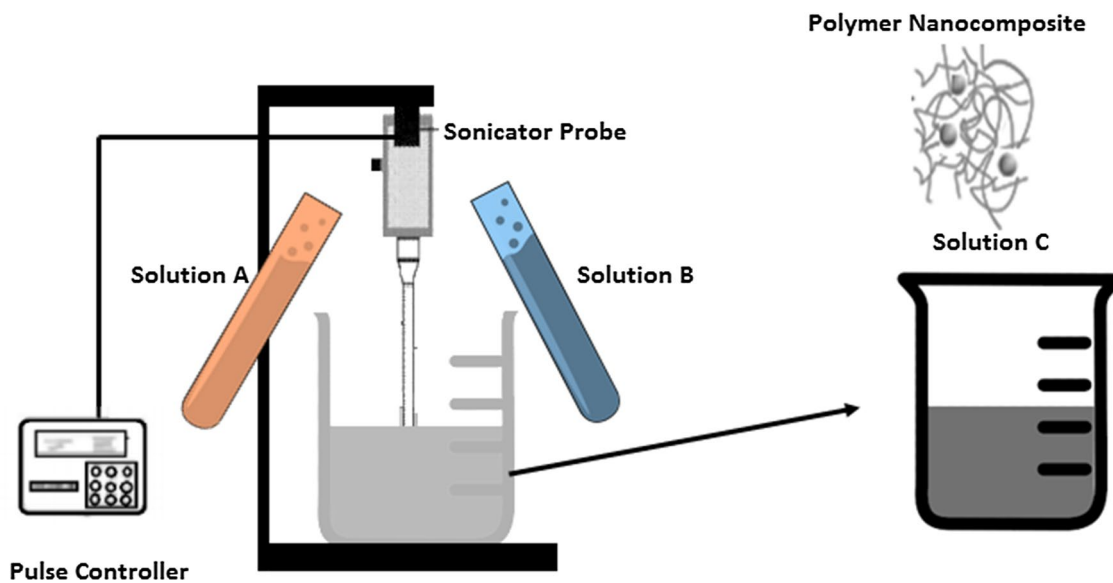
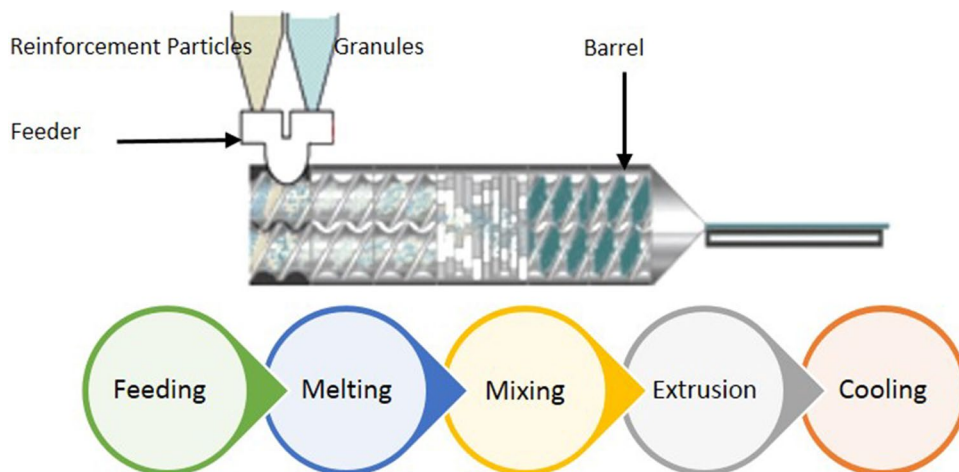


**Fig. 6** Ultrasound cavitation technique in which a solution containing a nanopolymer composite is prepared after mixing two solutions A and B, and then a sonicator probe is immersed, and using a pulse controller, ultrasound is applied

and temperature locally, with the overall ambient temperature of the environment. The subsequent formation of these cavities is called cavitation. By introducing ultrasound, the

cavitation energy can be used for the cracking of the petroleum residue.

**Fig. 7** Melt processing extrusion technique that involves direct mixing the host nanofillers with a polymer powder by a twin-screw extruder or blender, pressing the mixture into a pellet, and heating at the appropriate temperature



### Direct mixture of polymer and particulates

Direct mixing of nanoparticles with a polymer melt in technical polymer processes, such as extrusion, is a classical method for preparing composite materials from thermoplastic polymers. As illustrated in Fig. 7, the melt processing extrusion technique involves direct mixing the host nanofillers with a polymer powder by a twin-screw extruder or blender, pressing the mixture into a pellet, and heating at the appropriate temperature.

### Template synthesis

In this technique, a template is used to form nanocomposite materials of a particular shape, for example layered and hexagonal shape. The soluble polymer acts as a template for the formation of layers. The technique is based on self-assembly forces, and the polymer serves as a nucleating agent and promotes the growth of the inorganic filler crystals. As those crystals grow, the polymer is trapped within the layers and thus forms the nanocomposite. Generally, template synthesis is an easy procedure with large-scale production (Alexandre and Dubois 2000).

### Mechanical milling

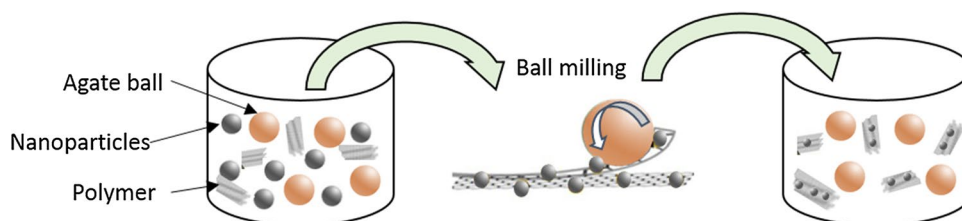
Mechanical milling is a well-established technique in polymer composite synthesis which involves continuous

mixing with repeated high-intensity plastic deformation. These deformations can provoke composites with atomic-scale dimensions. So, the main objective of this technique is to reduce the particle size and blend the particles in new phases. As illustrated in Fig. 8, the method involves the use of agate balls in a ball mill jar where the nanoparticles are milled simultaneously with the polymer to produce a polymer nanocomposite. Mechanical milling is solid-state mixing that enhances the homogeneous dispersion of filler into the polymer matrix and is a better ecological and economical alternative. It works at low temperatures and can be used for almost any type of polymer matrix. More advanced materials can be prepared when working at low temperatures, with any type of polymer, and without any extremely important solvent.

### Nonconventional methods

To facilitate better dispersion of the filler in the polymer matrix for improved properties of final composites, researchers investigated different routes based on the traditional methods mentioned previously. For instance, *in situ* polymerization can be customized to be redox or catalytic chain transfer or even photo-induced polymerizations. Others include microwave-induced synthesis, one-pot synthesis, template-directed synthesis, electrochemical synthesis, self-assembly synthesis, and intermatrix synthesis (IMS).

**Fig. 8** Ball milling technique involving the use of agate balls in a ball mill jar where the nanoparticles are milled with the polymer to produce a polymer nanocomposite



## Polymer composites for gamma-radiation shielding

### Development of polymer composites as gamma-radiation shielding materials

To improve the polymer performance and characteristics, a stiff material called filler can be added to the polymer matrix to form a polymer composite. The combination between filler and polymer matrix provokes the formation of a mixture that influences the polymer–composite properties by retaining the properties of both the filler and the polymer. The composite materials are named according to the reinforcement and the matrix material constituting them. There are many types of matrix materials such as metal matrix composites, polymer matrix composites, ceramic matrix composites, and epoxy resin matrix composites. The availability of radiation shielding materials that can be moulded into specific shapes and used even at high temperatures is quite significant for medical and industrial procedures.

The resistance of a material to radiation is attributed to many factors such as the type of radiation used, the rate of absorbed dose, radiation exposure (pulsed or continuous), area and size of the material, the surrounding environment (pressure, temperature, electric, or magnetic field) (McMillan 2019). But in inorganic materials, the radiation resistance depends on the type of chemical bond and crystal structure of the material (Wozniak et al. 2017). Due to relatively high processing ability and durability, polymer composite materials are vastly used in various fields of industry. Since 1916, the first polymer composite was used as phenol–formaldehyde resin (wood flour) by bakelite. Recently, about 10,000 fillers are known and used. The main duty of the filler is to provide the material with special properties and cost-effectiveness. Composites of polymer materials are superior due to their merits in flexibility, low cost, workability, mechanical stability, high aspect ratio. Also, the research studies confirmed that composite materials not only are better in radiation resistance but also have thermal stability and high mechanical properties (Zezin et al. 2004). Numerous studies are reporting the use of polymer composites as gamma-radiation shields.

Different barite concentrations 0%, 10%, 20%, 30%, 40%, and 50% were added to epoxy, and the linear attenuation coefficients of the composites increased with the increase in barite concentrations (Al-Sarray et al. 2017). Styrene-butadiene rubber (SBR-1502)/montmorillonite nanocomposites in the presence of ferric oxide ( $\text{Fe}_2\text{O}_3$ ), zinc oxide (ZnO), molybdenum oxide (MoO), and titanium dioxide ( $\text{TiO}_2$ ) were synthesized to investigate their effectiveness in shielding against gamma radiation. Styrene-butadiene rubber/molybdenum oxide (SBR/MoO) composite confirmed

the best performance as a radiation shield and its effectiveness in nuclear medicine departments (Atta et al. 2015). The gamma-rays radiation shielding properties for composites of natural rubber (NR) and styrene-butadiene rubber (SBR-1502) incorporated with different concentrations of the lead were investigated by using  $^{137}\text{Cs}$  as a gamma radiation source. The results confirmed that the linear attenuation coefficient  $\mu$  increased significantly with the increase in filler content (Gwaily 2002). Multiple ABS (acrylonitrile butadiene styrene) with different addition concentrations of bismuth ( $1.2\text{--}2.7\text{ g/cm}^3$ ) was synthesized and tested, and the radiation attenuation behavior was improved by increasing bismuth concentration (Ceh et al. 2017). Also, polylactic acid (PLA) nanocomposites containing 3%, 5%, and 7% zeolite were prepared by solution casting method. The increment in zeolite content promoted the increase in radiation resistance due to polymer interaction with radiation and the formation of reactive (Yildirim and Oral 2018). Gamma-ray shielding performance of 3-dimensional (3D)-printed poly-ether-ether-ketone/tungsten composites (Wu et al. 2020) and poly(vinyl alcohol)–bismuth oxide composites (Muthamma et al. 2019) for X-ray and gamma ( $\gamma$ )-ray shielding applications were investigated.

Polycarbonate (PC) loaded with different filler levels equal to 0.1, 0.2, 0.3, 0.5, 0.75, 1.0, 2.5, 3.5, and 5.0 wt% (weight percent) of bismuth nitrate pentahydrate ( $\text{Bi}(\text{NO}_3)_3 \cdot 5\text{H}_2\text{O}$  or BNP) was prepared via dispersing of filler in polycarbonate solution, followed by casting. The radiation attenuation parameters showed considerable variation with a strong dependence on the energy of the incident gamma-ray photon and the concentration of bismuth nitrate pentahydrate (BNP) incorporated as filler within the polycarbonate matrix (Mirji and Lobo 2020). Gadolinium oxide/poly-ether-ether-ketone ( $\text{Gd}_2\text{O}_3/\text{PEEK}$ ) composites were synthesized using a twin-screw extruder. The X-ray shielding properties of composites improved with the increment of the  $\text{Gd}_2\text{O}_3$  (gadolinium oxide) (Wang et al. 2015). Polyethylene/boron carbide composites were fabricated using conventional polymer processing techniques. The sample containing 2 wt% (weight percent) boron carbide composite showed the best radiation shielding measurements (Harrison et al. 2008). Photon shielding properties for bismuth oxychloride ( $\text{BiClO}$ ) 5, 10, 15, and 20% filled polyester concretes were studied in the energy range of 59.5–1408 keV using an HPGe detector. The experimental values are in good agreement with those obtained from XCOM and FLUKA code. In the prepared polymer composites, bismuth oxychloride (20%) filled polyester has the best radiation shielding property among the selected samples (Sharma et al. 2020). Gamma-ray and neutron shielding characteristics of polypropylene fiber-reinforced heavyweight concrete exposed to high temperatures were studied and barite concrete for simultaneously achieving better residual compressive

strength, gamma ray, and neutron shielding capability were recommended (Demir et al. 2020).

Four samples have been prepared by different proportions (5–20%) of filler materials (barium titanate, BaTiO<sub>3</sub>, and calcium tungsten oxide, CaWO<sub>4</sub>). Experimentally determined values of the linear attenuation coefficients, radiation protection efficiencies, half-value layers, mean free paths, and effective atomic numbers of studied polymer composites have been supported with theoretical results. Among the prepared polymer composites, barium titanate (20%) and calcium tungsten oxide (20%) have better gamma-ray attenuation characteristics than the other tested polymer composites. Calcium tungsten oxide, CaWO<sub>4</sub> (20%), has slightly better gamma-ray attenuation properties than barium titanate, BaTiO<sub>3</sub> (20%) (Akman et al. 2020). Gamma-ray attenuation characteristics of poly (methyl methacrylate) composites with 0–44 wt% of bismuth trioxide (Bi<sub>2</sub>O<sub>3</sub>) filler were investigated. The fast ultraviolet curing method was used for the preparation of polymer composites. The physical and mechanical properties of prepared polymer composites have also been studied. The high loading of bismuth trioxide in the polymethyl methacrylate (PMMA) samples improved the microhardness to nearly seven times that of the pure PMMA (polymethyl methacrylate) (Cao et al. 2020). Using NaI detector for gamma rays detection, the attenuation parameters of including the mass attenuation coefficient ( $\mu/\rho$ ), mean atomic number ( $\langle Z \rangle$ ), effective atomic cross section ( $\sigma_a$ ), effective atomic number ( $Z_{\text{eff}}$ ) plus electron number ( $N_{\text{eff}}$ ) for the samples: pure epoxy, aluminum oxide (Al<sub>2</sub>O<sub>3</sub>) epoxy (6 and 15 weight %), and ferric oxide (Fe<sub>2</sub>O<sub>3</sub>) epoxy (6 and 15 weight %), were determined. With the increase in gamma-ray energy, mass attenuation coefficient and effective atomic cross-section values were decreased, whereas effective atomic and electron number values were increased (Al-Dhuhaibat et al. 2020).

Gamma-ray shielding properties of polyester composite reinforced with different proportions of cadmium telluride (CdTe) have been investigated experimentally using HPGe detector and theoretically using XCOM program in the energy range of 59.5–1408.0 keV. Remarkable radiation protection efficiency was obtained by filler material cadmium telluride (Akman et al. 2021). Photon attenuation characteristics such as mass attenuation coefficient, half and tenth value layer, mean free path, effective atomic number and electron density, and buildup factors of polyvinyl alcohol (PVA) mixed with lead nitrate, Pb(NO<sub>3</sub>)<sub>2</sub> (0–30 weight%) were studied experimentally along with using XCOM values and MCNP5 simulations. With the increase in additive material, radiation shielding characteristics of polymer matrix were observed to be increased (Issa et al. 2019). A skin-interactive metal-free spongy electrode in the piezoelectric sensor was reported where highly aligned poly(vinylidene fluoride) (PVDF) nanofibers (NFs) arrays are introduced as

piezoelectric active component and conducting polyaniline-coated polyvinylidene difluoride (PANI-PVDF) nanofibers mats served as flexible electrodes. Ninety-nine percent yield of piezoelectric phases of the aligned polyvinylidene difluoride arrays is the key factor to exhibit promising mechano-sensitivity performance that in turn helps in human health monitoring (Maity et al. 2020). The radiation shielding properties of flexible polyvinyl alcohol/iron oxide polymer composite with five different concentrations of magnetite were investigated in the energy range of 15 keV–20 meV. 0.5% of the magnetite which gives superior shielding properties compared with other concentrations (Srinivasan and Samuel 2017).

For filler-enhanced materials, innovation has led to greatly improved properties and functions with nanofillers, which cannot be obtained using traditional macro- and microtechnology within normal filler loading levels. Filler-enhanced polymer nanocomposite technology is one of the driving forces in stimulating and promoting nanotechnology development and has attracted considerable interest in both academia and industry. At present, nanotechnology has expanded into almost every aspect of science and technology.

### Advances in polymer composites by the use of nanofillers

In general, the incorporation of nanofillers into the composite material leads to the enhancement of composite properties. The filler is bonded to the polymer matrix via weak chemical and intermolecular forces. But on the nanometer scale, a nanofiller can be dispersed within the polymer matrix. Thus, the molecular interactions between the matrix and the filler are improved via chemical bonding leading to further enhancement in the mechanical and physical properties of the new polymer nanocomposites (Kumar et al. 2009). The nanofillers are characterized by a high surface-to-volume ratio which causes the alteration in the macromolecular state around the nanoparticles. Promising features of the polymer are enhanced by the addition of nanofiller, such as increased elastic stiffness and strength, heat and barrier resistance, decreased gas permeability, and mainly radiation resistance. Also, nanoparticles offer a great advantage compared to other additives to the polymer since the loading requirements are quite low. Many factors can influence polymer nanocomposites including the type of filler, the ratio of the filler to matrix, synthesis technique, and its conditions. By dispersing nanofillers within a polymer matrix, an obvious enhancement in the composite properties is obtained.

Many polymers can be added as the base matrix, and polyethylene (PE) as an example is a widely used material in many applications; however, many environmental factors affect this polymer such as solar radiation,

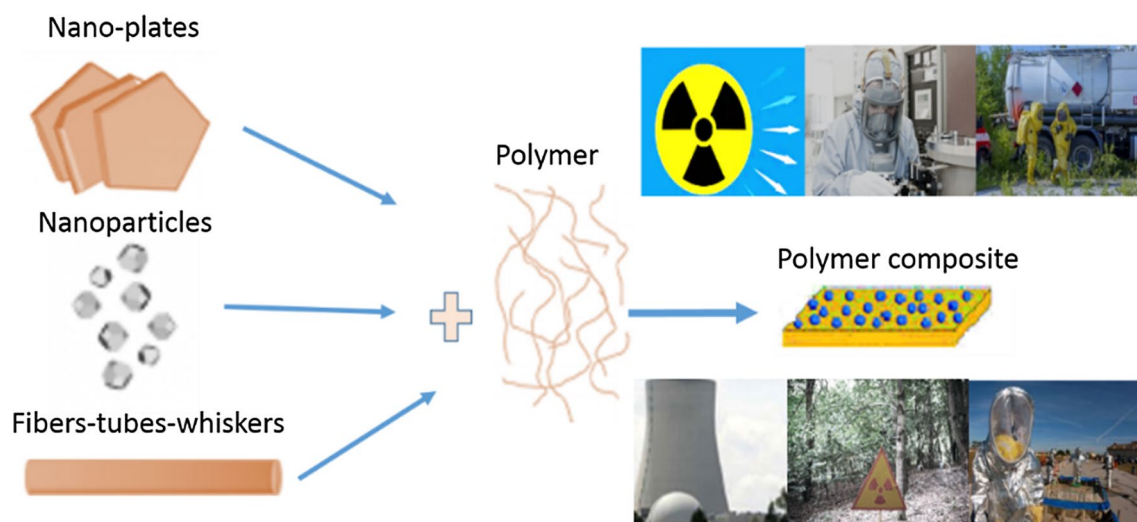


**Fig. 9** Many forms of nanoplates, nanoparticles, fibers, tubes, and whiskers can be added to polymer matrix to synthesize polymer composites which can be used as radiation shielding materials in radiation facilities, nuclear power plants, and also nuclear cleaning of environment

temperature, thermal cycling, humidity, weather, and pollutants. Other types of polymers such as low-density polyethylene (LDPE), high-density polyethylene (HDPE), polyvinyl alcohol (PVA), polystyrene (PS), polypropylene (PP), and polyvinyl pyrrolidone (PVP) are also important and widely used. An important feature that characterizes polymer nanocomposites is their good performance in radiation shielding. Protection and convenient shielding against ionizing radiation are essential to minimize the harmless effect on both humans and the environment. As illustrated in Fig. 9, many forms of nanoplates, nanoparticles, fibers, tubes, and whiskers can be added to polymer matrix to synthesize polymer composites which can be used as radiation shielding materials in radiation facilities, nuclear power plants, and also nuclear cleaning of environment. Various studies focused on the effect of adding nanofiller on the radiation shielding behavior of polymer composites. The incorporation of different types of fillers into the polymer matrices has shown interesting results in the attenuation of gamma radiation.

The incorporation of nanofillers mainly carbon-based and metal/metal oxide nanoparticles into polymeric membrane matrixes improved the filtration capability of nanocomposite membranes to separate pollutants from water which has been a global challenge due to the great demand for clean water supply (Wen et al. 2019). The degradation of fragmented microplastic residues containing low-density polyethylene (LDPE) via visible-light-induced heterogeneous photocatalysis enhanced by zinc oxide nanorods showed an increase in brittleness, cracks on the surface, and in carbonyl index of residues with a value of 30% (Tofa et al. 2019). High-density polyethylene (HDPE) composite loaded with tungsten (W), molybdenum disulfide ( $\text{MoS}_2$ ), and boron

carbide ( $\text{B}_4\text{C}$ ) demonstrated that the flexible composite sheet of high-density polyethylene/45% (wt) tungsten provided comparable X-ray absorption to the non-flexible lead sheet but much lighter in weight (Afshar et al. 2019). Micro- and nanosized tungsten oxide ( $\text{WO}_3$ ) were added to polyvinyl chloride (PVC) and studied against low energy X-rays, and nanostructured tungsten oxide/polyvinyl chloride shields have higher photon attenuation compared to the microsized samples (Aghaz et al. 2016). Cerium oxide ( $\text{CeO}_2$ ) nanoparticles were synthesized by the sol-gel method and were further used to develop polysulfone–cerium oxide mixed-matrix membrane with enhanced gamma radiation-resistant property (Bedar et al. 2019).

The gamma-ray attenuation parameters of high-density polyethylene/zinc oxide composite prepared via compression moulding technique by mixing bulk and nanozinc oxide of weight percent (10, 20, 30, and 40 weight %) with high-density polyethylene as a polymer matrix were studied. The results obtained for radiation shielding parameters of nanozinc oxide blended with high-density polyethylene were found to be more promising and efficient for radiation protection against gamma-ray. Mass attenuation coefficient, molecular, and atomic cross-section ( $\mu_m$ ,  $\sigma_{\text{mol}}$ , and  $\sigma_{\text{atm}}$ ) values decreased with incident photon energy and increased with the weight percentage of both bulk and nanozinc oxide filler (Alsayed et al. 2019, 2020). Epoxy composite samples filled with lead oxide ( $\text{PbO}$ ) and lead tetraoxide ( $\text{Pb}_3\text{O}_4$ ) were fabricated to investigate the mass attenuation characteristics of the composites to X-rays in the diagnostic imaging energy range. The effect of density on the attenuation ability of the composites for radiation shielding purposes was studied using a calibrated X-ray machine (Azman et al. 2013). By varying the amounts of powdered fillers

lead oxide (PbO) and tungsten oxide (WO<sub>3</sub>) added to low density-polyethylene, the attenuation performance against gamma radiation was studied revealing that the samples of high filler loadings showed good attenuation performance against gamma radiation (Belgin and Aycik 2015). Also, zirconium dioxide (ZrO<sub>2</sub>) nanoparticles with various weight percent (1, 2, 3, 5, and 10 wt%) were added to synthesize poly(vinylidene fluoride–trifluoroethylene)/zirconium dioxide [P(VDF-TrFE)/ZrO<sub>2</sub>] polymer composites and investigate their protective shielding of patients during radiological procedures (Fontainha et al. 2016).

Ultra-high-molecular-weight polyethylene (UHMWPE) fiber epoxy composite hybridized with gadolinium, boron nanoparticles (Mani et al. 2016), and nanoe epoxy (Zhong et al. 2009) showed good neutron shielding performance. Moreover, high-density polyethylene/bismuth (HDPE/Bi) composite prepared by adding different weight percentages (0%, 10%, 20%, and 40%) of bismuth in high-density polyethylene (HDPE) matrix showed the shielding efficiency of synthesized high-density polyethylene/bismuth composites increases with an increase in the weight percentage of bismuth (Sheela et al. 2019). The physicochemical properties of low-density polyethylene and ethylene–vinyl acetate composites cross-linked by ionizing radiation by melt mixing showed that low-density polyethylene/ethylene–vinyl acetate copolymer/carbon black (LDPE/EVA/CB) and ethylene–vinyl acetate copolymer/carbon black (EVA/CB) composites tend to crosslink by irradiation (Basfar and Ali 2011). Using Ba-133, Cs-137, and Co-60 gamma-ray sources, the effect of adding bismuth oxide as a reinforcement to unsaturated polyester was investigated, revealing that by increasing filler content, the radiation shielding properties increase. The half and tenth value layer and relaxation length of the composites were found to decrease with an increase in the filler concentration (Ambika et al. 2017). Nanotungsten (W) dispersed polymer composite was significant 75% for 133Ba ( $\approx 0.3$  MeV) compared to the microtungsten (W) composites (Das et al. 2009), and also silicone rubber matrix dispersed with 37.5% weight of tungsten (W) and bismuth oxide (Bi<sub>2</sub>O<sub>3</sub>) confirmed good gamma-ray-shielding performance compared to lead (Atashi et al. 2018). Tungsten oxide (WO<sub>3</sub>) and bismuth oxide (Bi<sub>2</sub>O<sub>3</sub>) nanoparticles improved the radiation shielding properties of hematite–serpentine concrete (HSC) (Tekin and Issa 2018) and emulsion polyvinyl chloride (EPVC) (Shik and Gholamzadeh 2018).

The effect of adding lead (Pb) powder to natural rubber (NR) and wood/natural rubber composites was investigated, and their performance in radiation shielding was efficient in attenuating low-intensity gamma rays (Ninyong et al. 2019). Iso-phthalate-based unsaturated polyester resin filled with different concentrations of lead monoxide particulate polymer composites was prepared for gamma rays of energy 0.662 MeV from <sup>137</sup>Cs point source, and linear attenuation

coefficient was found to increase with increased filler content in the composites (Harish et al. 2012). The radiation shielding properties of concrete were improved for gamma rays of 662, 1173, and 1332 keV using <sup>137</sup>Cs and <sup>60</sup>Co sources via adding nano lead compounds (Hassan et al. 2015). Nanogadolinium oxide (Gd<sub>2</sub>O<sub>3</sub>) composites were more efficient in shielding X- and gamma ray than microgadolinium oxide (Gd<sub>2</sub>O<sub>3</sub>) composites, and an enhanced effect of  $\sim 28\%$  was obtained with gadolinium oxide (Gd<sub>2</sub>O<sub>3</sub>) content of around 5 weight percent at 59.5 keV (Li et al. 2017). The addition of micro- and nanocadmium oxide (CdO) particles to the high-density polyethylene matrix increased the mass attenuation coefficients of the composites mainly at low gamma-ray energies (El-Khatib et al. 2019). The polymer–matrix composites based on high-density polyethylene with either lead oxide (PbO) nanoparticles or lead oxide bulk using 10 and 50% weight fractions synthesized by solid-state intermixing and thermal pressing technique showed interesting gamma-rays shielding properties especially for high filler loadings (Mahmoud et al. 2018a, b).

X- and gamma-rays attenuation parameters for polyacrylamide and zinc oxide (ZnO) composites were evaluated as light-shielding materials using MCNP and XCOM simulation. The obtained results showed that the composites were better in gamma-ray shielding performance compared to the bulk of zinc oxide (Nasehi and Ismail 2019). Extensive investigation on gamma-ray shielding features of palladium/silver (Pd/Ag)-based alloys in the energy range 81 keV–1333 keV by using an HPGe detector, revealing that palladium/silver (Pd75/Ag25) alloy sample had superior photon shielding characteristics among all composites (Agar et al. 2019). Unsaturated polyester containing 5 weight percent nanoclay and different amounts of lead monoxide particles (0, 10, 20, and 30 weight percent) were investigated by <sup>192</sup>Ir, <sup>137</sup>Cs, and <sup>60</sup>Co gamma radiation sources, the mass, and linear attenuation coefficients which were increased by increasing lead monoxide content (Bagheri et al. 2018). The radiation shielding performance of natural fiber high-density polyethylene and lead oxide composites revealed that the mass attenuation value decreased sharply from 10 keV to 0.8 MeV and then smoothly decrease above 0.8 up to 15 MeV (Abdo et al. 2003). Nanostructured natural bentonite clay coated by polyvinyl alcohol polymer materials (Hager et al. 2019) were developed for gamma rays attenuation.

The radiological parameters of composite filler, zirconium, and acrylic coating materials used in dental treatment revealed that maximum attenuation occurred for samples of 1 mm thickness where 21%, 10%, and 2% of the incident radiation were absorbed by zirconium, composite, and acrylic samples, respectively (Abbasova et al. 2019). The attenuation coefficients against gamma radiation were studied for polyvinyl alcohol–polyethylene glycol–polyvinyl pyrrolidinone with zirconium oxide (PVA–PEG–PVP–ZrO<sub>2</sub>)

nanocomposites which showed to increase with zirconium oxide content (Agool et al. 2017). Also, tungsten/bismuth oxide/methyl vinyl silicone rubber (W/Bi<sub>2</sub>O<sub>3</sub>/VMQ) composites exhibited higher X-ray-shielding properties in the X-ray energy ranging from 48 to 185 keV (Chai et al. 2016). Ultra-high-molecular-weight polyethylene (UHMWPE) with boron carbide, B<sub>4</sub>C, and tungsten, W, nanopowders were fabricated by solid-state intermixing and thermal pressing, and the gamma protection properties increased with tungsten content in the composite (Kaloshkin et al. 2012). Polymer composites with different aluminum oxide percentages ( $x=0, 10, 20, 30, 40,$  and 50 weight percent) were prepared, and the composites of 40 weight percent (wt%) aluminum oxide (Al<sub>2</sub>O<sub>3</sub>) revealed the highest values of radiation attenuation (Osman et al. 2015). Bismuth nanoparticles with cellulose nanofibers and polydimethylsiloxane (PDMS) polymer can effectively shield X-ray radiation at a lower mass ratio in the polymer matrix (Li et al. 2018). Novel polyvinyl alcohol (PVA)/tungsten oxide (WO<sub>3</sub>) composite consisting tungsten oxide (WO<sub>3</sub>) at sizes of 10 μm and 30 nm with a weight concentration of 50 weight % was studied for gamma-ray shielding (Kazemi et al. 2019).

The polyacrylamide (PAGAT) gel and metal nanoparticle (different concentrations of gold and silver) verified the water equivalency based on an effective atomic number (Sathiyaraj et al. 2017). Different percentages of tungsten carbide (50, 60, and 70%) were added and tested against gamma radiation (<sup>137</sup>Cs and <sup>131</sup>I and <sup>241</sup>Am), and the best shielding efficiency against gamma radiation was revealed by the composite with 70% tungsten carbide (WC) (Soylu et al. 2015). Different percentages of tungsten carbide (50, 60, and 70%) were added and tested against gamma radiation (<sup>137</sup>Cs and <sup>131</sup>I and <sup>241</sup>Am), the best shielding efficiency against gamma radiation was revealed by the composite with 70% tungsten carbide (Özdemir et al. 2018). Graphite/epoxy composite showed the highest performance in gamma radiation attenuation among epoxy/graphite, epoxy/lead, and epoxy/boron (Saiyad et al. 2014). A proportional relationship between photon attenuation coefficients and barite concentration was revealed when barite and boron carbide-doped radiation shielding polymer composite was prepared for radiation shielding (Evcin et al. 2017). Blended powdered polyethylene glycol and lead oxide prepared by physical mixing revealed that the shielding properties of polyethylene glycol increased with the addition of lead oxide (Hussain et al. 1997).

The influence of bismuth contents on mechanical and gamma-ray attenuation properties of silicone rubber composite was studied, showing that the increase in bismuth content induced an increase in radiation shielding performance (El-Fiki et al. 2015). Four different colemanite Ca<sub>2</sub>B<sub>6</sub>O<sub>11</sub>·5H<sub>2</sub>O (CMT) concentration levels (such as 5, 15, 30, and 40 weight percent) were examined to investigate

the radiation protective shielding properties of poly(methyl methacrylate)/colemanite (PMMA/CMT) composite. Colemanite reinforcement of poly(methyl methacrylate) increased the radiation shielding capacity by 11.1% for gamma photons of Cs-137 radioisotope (Bel et al. 2018). By blending epoxy resin with different weight percent of tungsten powder, tungsten/epoxy composites were prepared and investigated by using two different activities of Co-60 source showing that with the increment of tungsten loading, the shielding property of composites increased (Chang et al. 2015). Besides, ethylene–vinyl acetate (EVA)–tungsten composite (Yurt Lambrecht et al. 2016) and polyimide/bismuth oxide (Pavlenko et al. 2019) composites revealed high radiation-protective characteristics. The shielding effect and the protective properties of the samples of aluminum alloys with a protective coating were evaluated revealing that tungsten–aluminum oxide (W–Al<sub>2</sub>O<sub>3</sub>) and tungsten–boron nitride (W–BN) coatings contribute significantly to the attenuation of ionizing radiation fluxes (Vilkov et al. 2017). Poly (lactic acid) (PLA) nanocomposites containing 3%, 5%, and 7% zeolite were prepared and investigated against gamma radiation at the absorbed doses of 10, 15, and 20 kGy. The results revealed that increasing zeolite content in the structure promoted the recombination of the reactive species formation with the interaction of the radiation in the polymer and increased the radiation resistance (Yildirim and Oral 2018).

Silica nanoparticles combined with composites are widely used for various applications (Soundharraj et al. 2020) such as glucose biosensors when combined with gold nanoparticles to form mesoporous silica composite, by incorporating silica nanoparticles to carbon dots for bioimaging applications, in drug delivery when mesoporous mobil composition of matter (MCM)-41-silica is loaded with ibuprofen, mono-dispersed silica with uniform hollow-core mesoporous shell carbon nanospheres for supercapacitor applications. Different types of metal and metal oxide nanoparticles including silver, copper, palladium, zinc oxide, magnesium oxide, tin oxide are synthesized with various polymers and used for antimicrobial activity, food packaging, and improving shelf-life of food (Rai et al. 2018). Carbon-based nanostructures such as semiconductor compounds and polyoxometalates are used for water purification (Lopes et al. 2021).

## Recycling of polymers

Materials that have reached their end of life after primary use or of no use must be dismissed, and materials that remain from production are considered waste. Plastic waste is a part of this term. The primary constituents of municipal, industrial, and agricultural plastic wastes are generally thermoplastics because of the large volume and low cost of these materials such as high-density polyethylene,

polypropylene, ethylene–propylene copolymer, polystyrene, low-density polyethylene, polyamide, polyethylene terephthalate, polyvinyl chloride, and these thermoplastics can be recycled. Besides, it consists of small amounts of thermosets like epoxy resins and polyurethane rubber and these thermoset plastics cannot be recycled (Miskolczi et al. 2004). Nowadays, the Covid-19 pandemic has posed a huge plastic pollution worldwide, which lead to urgent and massive use of fossil fuel-derived plastic (Sorrentino et al. 2020).

Plastic wastes are a mixture of different types of plastics along with some contaminations. Microplastics which are considered plastic particles smaller than 5 mm represent slowly degrading contaminants in soil and water exposing human health and environment to toxic incorporation of these materials (Padervand et al. 2020). Also, this waste is big in volume, and for the waste management of plastic waste, an integrated waste management approach is needed. There are three ways for disposal of municipal and industrial plastic waste: incineration (with or without energy recovery), landfilling, and recycling. The incineration method for plastics wastes is always accompanied by the emission of harmful, greenhouse gases. More energy is dissipated in the process of plastic incineration. Also, landfilling is not an efficient technique because suitable and safe deposits are expensive (Grigoriadou et al. 2011). Thus, recycling is the best way to manage plastic wastes since it reduces environmental impact, resource depletion, and pollution. Besides, recycling of the plastics consumes a smaller amount of energy when compared to energy consumption in new virgin resin production. Fundamentally, high levels of recycling, as with a reduction in use, reuse, and repair or re-manufacturing can allow for a given level of product service with lower material input that would otherwise be required. Therefore, recycling can decrease energy and material used per unit of production and so yield improved eco-efficiency (Hamim et al. 2016).

Recycling can be divided into two categories: mechanical recycling and chemical recycling (Miskolczi et al. 2004). Chemical recycling is virtually a thermal method by which the long alkyl chains of polymers are broken into a mixture of lighter hydrocarbons. Several chemical reactions such as pyrolysis, cracking, glycolysis, and gasification can be used for the decomposition of polymers (Lee et al. 2002), whereas mechanical recycling is a physical method. It usually consists of contamination removal of the plastic wastes by sorting and washing, followed by grinding or conversion into flakes, granulates, or pellets, then drying, and melt processing to make the new product by extrusion. It is noted that mechanical recycling is the better method for recycling as is relatively simple, environmentally friendly, and requires low investment (Awaja and Pavel 2005).

Collection of post-consumer plastic wastes, separation, processing (manufacturing), and marketing are the four steps in plastic recycling (Shent et al. 1999). Different types of

polymers need to be separated from each other from the collected plastics waste to get better quality of recycled plastic. Several techniques can be used to separate mixed plastic wastes based on their physicochemical properties such as gravity separation, contact charging, hydro-cyclones and centrifuges, and froth flotation (Pascoe 2003). The produced recycled plastic can be used to manufacture new products such as automobile parts, floor carpets, flower vases, park benches, picnic tables, waste paper baskets, crates, plastic lumber, wood–plastic composites which will provide an additional market for recycled plastics. Sustainable and low-cost radiation shielding materials can be fabricated using composite materials from post-consumer recycled thermoplastics for various applications such as space, industry, and radiation facilities as shown in Fig. 10 (Cholake et al. 2017; Mahmoud et al. 2018a, b). Massive amounts of polyethylene terephthalate, high-density polyethylene, polyvinyl chloride, low-density polyethylene, polypropylene, polystyrene, and miscellaneous plastics can be recycled to fuels via many thermomechanical technologies including pyrolysis, liquefaction, and gasification (Nanda and Berruti 2020). Cellulose nanoparticles were extracted from conventional and nonconventional lignocellulosic biomass for food packaging applications to avoid the extensive use of nonbiodegradable materials. The synthesized cellulosic nanocomposites exhibited promising optical, biodegradation, mechanical, and barrier properties due to the large surface area of nanoscale structure (Qasim et al. 2020). Nanomaterials play also an important role in moisture absorbing packaging in food industry taking into consideration all the safety concerns and toxicity issues (Gaikwad et al. 2018). Cerium dioxide and composites are used as adsorbents for water decontamination to remove contaminants such as arsenic, fluoride, lead, and cadmium (Olivera et al. 2018).

### The use of processed and post-consumed polymers as composite materials for different applications

The world's main focus nowadays is the use of new materials that are eco-friendly to reduce the burden of pollution via recycling these materials and enhancing their sustainability. This urged the need and synthesis of new composite materials via adding fillers as alternatives for replacing toxic and harmful fabricated materials. New attempts to process and refine post-consumed polymers are obtained. Many researchers are concerned about the use and processing of composite materials for various types of applications.

Iron-based magnetic (Marcelo et al. 2020) and silver–magnetic nanocomposites (Surendhiran et al. 2017) are of great importance as they display promising performance in removing pollutants from water, adsorption of heavy metal ions, photocatalysis, soil conditioning (Sharma et al. 2018), and many other applications such as optical

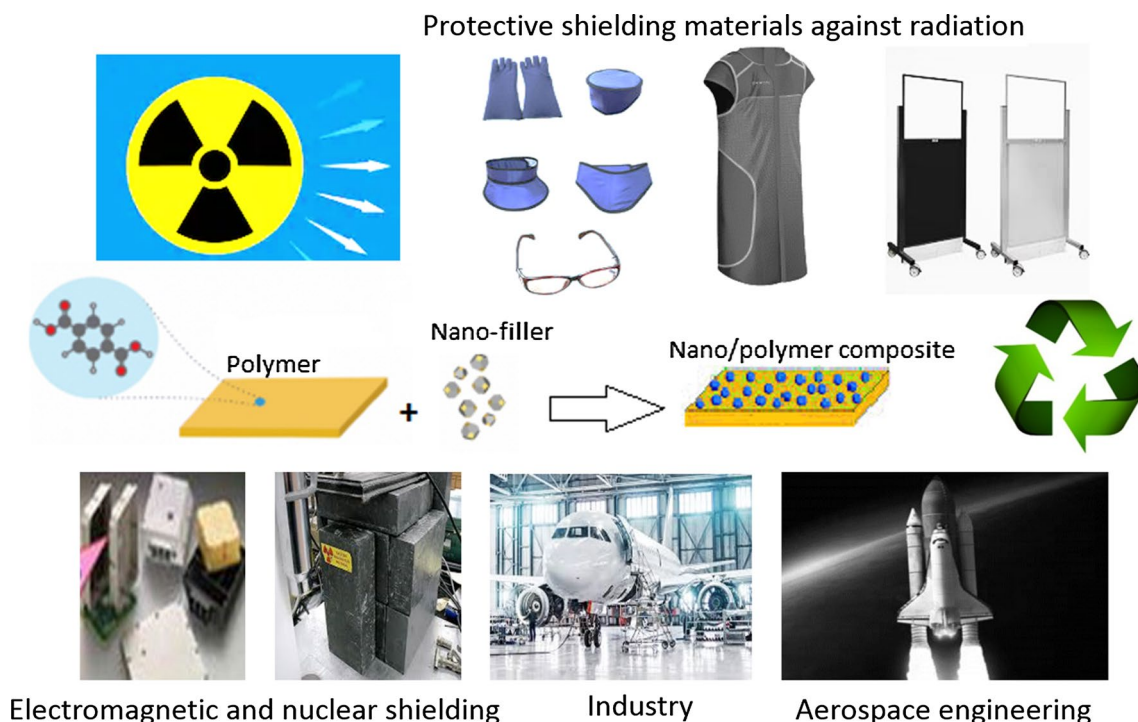


**Fig. 10** Use of polymer composite materials after recycling in various applications such as protective shielding materials in radiation facilities, aerospace engineering, industry, electromagnetic, and nuclear shielding

application, hydrogen storage, magnetic resonance imaging, and cancer diagnosis (Siddiqui et al. 2018). Also, the use of thermosets, fabrics, and textiles-based materials as polymer matrices has been extensively reported and investigated. Conversion of waste-derived high-density polyethylene to three-dimensional (3D) printing filament has important technological implications. A facile strategy to expand the palette of waste-derived polymer materials for fused filament fabrication (FFF) three-dimensional (3D) printing was explained in details (Gudadhe et al. 2019). The polymer–matrix composites based on recycled high-density polyethylene with either lead oxide nanoparticles or lead oxide bulk using 10 and 50% weight fractions were synthesized by solid-state intermixing and thermal pressing technique. This study suggests that the recycled high-density polyethylene/lead oxide nanocomposites could be used as sustainable gamma-radiation shields and these composites of the recycled polymer are environmentally effective (Mahmoud et al. 2018a, b).

Banana/E-glass fabrics fabricated by reinforcing polyester hybrid composites were evaluated. The maximum hardness and tensile strength were attributed to pure glass fabric laminate, whereas minimum values were attributed to pure banana fabric laminate. The mechanical properties of the synthesized materials were enhanced by the addition of the glass layer. The maximum absorption of water was established by pure E (electrical)-glass fabric laminate

(Sanjay et al. 2016). The performance of polyurethane-based composites prepared from recycled polymer concrete via adding ethylene–vinyl acetate (EVA) was investigated, the mechanical and durability of the composite were enhanced by increasing ethylene–vinyl acetate content. The performance of polyurethane-based composites is prepared from recycled polymer concrete via adding ethylene–vinyl acetate (EVA). They found that the mechanical and durability of the composite were enhanced by increasing ethylene–vinyl acetate (Ma et al. 2020). A combination of recycled polyethylene terephthalate (PET) fibers and epoxy/calcium carbonate ( $\text{CaCO}_3$ )-stearic acid composites was prepared, the optimal content for calcium carbonate ( $\text{CaCO}_3$ ) particle modification was 2 wt% (weight percent), and the thermal stability and mechanical properties were improved (Nguyen et al. 2020). Different wt% (weight percent) of coal mining waste (CMW) were added to synthesize coal mining waste/low-density polyethylene (CMW/LDPE) composite and study the eco-toxicological effects in water and soil. The results confirmed that a 50% increment in the pH value was for the leachate of 20% weight low density polyethylene composite with a noticeable reduction in the eco-toxicological effect (Gryczak et al. 2020).

The recycled filaments of continuous carbon fiber and polylactic acid (PLA) matrix showed a high tensile performance with high bending strength. Due to the special properties of three-dimensional printed carbon fiber-reinforced

thermoplastic composites (CFRTPCs), high material recovery rates were observed for the polylactic acid matrix (73%) and carbon fiber (100%) (Tian et al. 2016). Recycled polyethylene terephthalate and polyacrylonitrile (RPET/PAN) composites showed a flexural strength increment and drying shrinkage (Chinchillas-Chinchillas et al. 2019). The chemical oxygen demand (COD) was reduced, and the mineralization percentage in recycled polymeric materials include cotton, cotton lycra, polyamide, paper, polyethylene terephthalate, polypropylene, and polyurethane (El-Mekkawi et al. 2019). The incorporation of phosphate tailings (PT) and fly ash (FA) reduced the thermal degradation temperature, smoke production rate (SPR), total heat release (THR), and the emissions of toxic carbon dioxide (CO<sub>2</sub>) and carbon monoxide (CO) in thermoplastic polyurethane (TPU) to fabricate polymer materials having minimal fire hazards via the solvent blending method (Zhou et al. 2020). Compared to sodium silicate–concrete waste (Na<sub>2</sub>SiO<sub>3</sub>–CoW), the addition of 10 weight percent lead-bearing sludge (LBS) in sodium hydroxide–concrete waste (NaOH–CoW) enhanced the mechanical properties of concrete waste (CoW) (Abdel-Gawwad et al. 2020). Maximum water absorption was attained by the high contents of recycled newspaper fiber (RNF) composites. The incorporation of metaled polypropylene (MAPP) had an interesting effect on enhancing the adhesion quality between fibers and polymers (Ashori and Sheshmani 2010).

Maleic anhydride-modified polypropylene/desulfuration modified recycled rubber (M-PP/M-RR) revealed an important increase in the mechanical properties compared to recycled rubber (RR) (Chiang et al. 2020). Also, the addition of silicon dioxide (SiO<sub>2</sub>) improved the mechanical properties of polyethylene terephthalate/poly(acrylonitrile butadiene styrene) (PET/ABS) (Shi et al. 2011). The interfacial compatibility between high-density polyethylene and wood flour via incorporation of metaled polypropylene (MAPP) as well as flexural strength and stiffness was improved (Adhikary et al. 2008). Also, by increasing fiber loading of microcrystalline cellulose (MCC) from (2–50 weight %), the tensile strength of recycled polypropylene/microcrystalline cellulose (PP/MCC) composites decreased, with an increase in young's modulus (Zulkifli et al. 2015). Moreover, by increasing fiber loading (0–15 weight %), enhancement in the tensile strength of recycled polyethylene terephthalate (RPET)/maleic anhydride-grafted poly styrene–ethylene–butadiene–styrene (SEBS-g-MA)/date palm leaf fiber composite was observed (Dehghani et al. 2013). Also, by increasing bamboo fiber content in the recycled talc-filled polypropylene/ethylene–propylene–diene monomer (EPDM) (Inacio et al. 2017) and due to the addition of talc in recycled polyethylene terephthalate/basalt fiber composite (Kráčalík et al. 2008), the flexural strength, tensile strength, and fatigue of composites increased. Due to the addition of graphite,

mica, and talc, the impact strength of kenaf wood recycled polyethylene was enhanced as well as the glass transition temperature of recycled plastic composite, WrPC (Ramli et al. 2018).

By increasing silica nanoparticles content to 1.0 weight %, the tensile properties increased and then decreased above this value. The highest obtained values of elongation at break, tensile modulus, and stress at break were revealed by unsaturated polyester resin (UPR)/vinyl silane silica nanocomposite (Rusmirović et al. 2016). The depolymerization process was used to recycled polyethylene terephthalate/dipropylene triethylene glycol and fabricate unsaturated polyester resin (UPR). The mechanical behavior of the composite after adding various wt% of graphite powder (GP 10 weight %), TiO<sub>2</sub> (10 weight %), and modified clay CLOISITE 30B revealed that by addition of graphite powder or titanium dioxide (TiO<sub>2</sub>), the composite showed better tensile properties (Marinkovic et al. 2013). By incorporating O-hydroxybenzene diazonium chloride (OBDC), silane, and glycidyl methacrylate (GMA) in sisal fiber-reinforced recycled polypropylene composites, the mechanical properties of the composite were preferably enhanced by O-hydroxybenzene diazonium chloride (OBDC)/recycled polypropylene composites (Gupta et al. 2014). Various amounts of clay content (Cloisite 10A 1 to 6 weight %) were added to recycled polyethylene terephthalate/clay nanocomposites. Impact strength remained intact up to 4 weight % and then decreased at 6 weight % and tensile properties were increased (Chowreddy et al. 2019). Alphazirconium hydrogen phosphate (ZrP) with the aid of chemically inert polymer coated with a titanium platinum electrode was used to collect harmful cobalt ions which are used as primary coolant in a nuclear power plant (Rathi and Ponnusamy 2020).

## Polymers for neutron shielding

It is infamous that the light atoms such as hydrogenous materials are more effective at shielding fast and intermediate neutrons for their competency of neutron moderation as light atoms slow down the neutrons through elastic scattering. Thus, water is preferred for neutron shielding. But it has the drawback of being in a liquid state at room temperature. Thus, polymer materials have a greater chance of shielding neutrons. The fast neutron removal cross section (cm<sup>-1</sup>) is the important characteristics to decide the fast neutron shielding capabilities of a material and is defined as the probability that a fast or fission energy neutron undergoes a first collision, which removes it from the group of penetrating, un-collided neutrons (Blizard and Abbott 1962).

There are several methods for the calculation of fast neutron removal cross section of materials. The conventional method for the quantitative determination of ( $\Sigma_R$ ) (cm<sup>-1</sup>) for fast neutrons is based on manual calculations and is applied

for several materials and composites (Glasstone and Sesonske 2012). The values obtained manually for fast neutron removal cross section are in good agreement (within about 10%) with values determined experimentally (El-Khayatt 2010). El-Khayatt and Abdo have developed MERCSEF-N program for the calculation of fast neutron removal cross sections for materials (El-Khayatt and Abdo 2009). The results of the MERCSEF-N program were validated with previously published results and confirmed a good agreement. El-Khayatt has developed an NXcom program for the determination of the removal and attenuation coefficients of transmitted fast neutrons and  $\gamma$ -rays, respectively (El-Khayatt 2011). Mass attenuation coefficient values calculated using the NXcom program have been confirmed by comparing them with the results of the WinXCom program. The NXcom program is a simple and easy method for the determination of neutron shielding performance. The effective fast neutron removal cross sections ( $\Sigma_R$ ) can be determined using the NXcom program (Yilmaz et al. 2011; Cataldo et al. 2019). There are some studies reported on the use of polymers as efficient neutron shielding materials (El Abd and Elkady 2014; Elmahroug et al. 2014; Jumpee and Wongsawaeng 2015; Mann et al. 2015a, b; Elwahab et al. 2019; Kaçal et al. 2019; Abdalsalam et al. 2020).

## Comparison

The most widely used materials are polymer materials and polymer composites due to their unique characteristics such as thermal-electrical insulation, corrosion resistance, mechanical and radiation shielding properties. However, many environmental issues concerning the use of such materials is rising pollution rates due to the effects of plastic residues which are gathered in nature and landfills (Hopewell et al. 2009).

Various strategies have been developed towards using and recycling polymer materials and their composites via different processes to maintain eco-friendly and recyclable materials. The main concern of researchers all over the world is to develop and synthesize new materials that would enhance their quality of being eco-friendly and environmentally sustainable. To reduce the negative impact of solid wastes on the environment, researchers were extremely motivated to increase their efforts towards using sustainable and recyclable materials (Liikanen et al. 2019). Based on the characteristics of the produced waste, two types can be categorized: hazardous and nonhazardous waste. Hazardous waste contains materials that have detrimental effects on humans and the environment (Ma et al. 2018).

Great attempts have been dedicated to using recycled polymers and polymer composites in many applications mainly as radiation shielding materials against harmful types of ionizing radiation. A brief comparison is done between

the mass attenuation coefficients of some polymers and their reinforced composites which reveal the importance of filler addition in improving the shielding behaviour of polymer-composite materials. Table 2 illustrates the comparison in mass attenuation coefficients of polymer materials and their composites. Also, few polymer-composite materials which revealed significant radiation shielding performance were compared to concrete in terms of mass attenuation coefficient and half-value layer as illustrated in Figs. 11 and 12, respectively. Figure 11 shows the values of mass attenuation coefficients of some polymer-composite materials compared to concrete at energy 661.66 keV. The composites (20% hematite/polystyrene, 50% lead oxide/polystyrene, 50% lead oxide/high-density polyethylene, and 40% zinc oxide/high-density polyethylene) were chosen based on their high performance of shielding against gamma radiation. The graph confirms that the polymer-composite materials having high amounts of fillers are more likely to attenuate gamma radiation compared to low amounts of fillers. Consequently, the presence of nanoparticles that have a high surface-to-volume ratio as fillers increases the probability of interaction between the photon beam and the composite. Also, the fillers have high electron density and can be uniformly distributed within the polymer matrix, thus enhancing the attenuation mechanism.

Figure 12 reveals the values of another important parameter for selecting the best material in radiation shielding, the half-value layer (HVL). The composites (50% hematite/polystyrene, 50% lead oxide/high-density polyethylene, 20% zinc oxide/polyacrylamide (PAM), and 40% zinc oxide/high-density polyethylene) were chosen based on their lowest values of half-value layer (HVL) since the lowest half-value layer (HVL) values are attributed to better shielding materials. Half-value layer (HVL) is a frequently used parameter that describes the penetration of radiation through objects and also the penetration ability. The fillers used have high densities so that the values of half-value layer decrease by increasing filler loading and are compared to concrete.

Table 3 shows the comparison between polymer materials and other materials such as glasses, flay ash bricks, alloys, and concretes in terms of macroscopic removal cross sections ( $\Sigma_R$ ). For the comparison, the material with higher values of macroscopic removal cross sections among the studied materials has been chosen. For example, 8 different fly ash bricks with varying compositions have been studied (Singh and Badiger 2013). Among these 8 different studied samples, fly ash brick sample 1 shows the higher values of  $\Sigma_R$  and that has been taken for comparison. Polymer materials have higher values of  $\Sigma_R$  than fly ash bricks, bismuth tellurite and bismuth boro-tellurite ( $(\text{TeO}_2)_{49}(\text{B}_2\text{O}_3)_{21}(\text{Bi}_2\text{O}_3)_{30}$  glasses, leaded brass alloys, some ordinary concrete. Thus, it can be concluded that polymer materials are better neutron absorbers.

**Table 2** Comparison between mass attenuation coefficients of polymer materials and their composites

S. n.o	Authors	Material	Mass attenuation coefficient $\mu_m$ ( $\text{cm}^2\text{g}^{-1}$ )				
			59.53 keV	80.99 keV	356.01 keV	661.66 keV	1173.25 keV
1	(Atta et al. 2015)	Control	–	–	–	0.0020	–
		Styrene butadiene rubber (SBR-1502)/montmorillonite + titanium(II) oxide	–	–	–	0.0258	–
		Styrene butadiene rubber (SBR-1502)/montmorillonite + ferric(III) oxide	–	–	–	0.0262	–
		Styrene butadiene rubber (SBR-1502)/montmorillonite + zinc(II) oxide	–	–	–	0.0284	–
		Styrene butadiene rubber (SBR-1502)/montmorillonite + molybdenum(II) oxide	–	–	–	0.0304	–
2	(Sharma et al. 2020)	Bismuth oxychloride-filled polyester concretes (5%)	0.3787	0.2539	0.1067	0.0804	0.0604
		Bismuth oxychloride (10%)	0.5710	0.3449	0.1182	0.0798	0.0644
		Bismuth oxychloride (15%)	0.6784	0.4148	0.1261	0.0851	0.0605
		Bismuth oxychloride (20%)	0.8273	0.4819	0.1253	0.0848	0.0638
3	(Mahmoud et al. 2018a, b)	High-density polyethylene	0.170	0.159	0.102	0.079	0.060
		50% Nano lead-oxide/high-density polyethylene	2.717	1.262	0.222	0.114	0.073
4	(Akman et al. 2020)	10% Lead(II) iodide/polyester	0.716	0.412	0.111	0.082	0.061
		20% Lead(II) iodide/polyester	1.165	0.628	0.120	0.0849	0.058
5	(Buyukyildiz and Kurudirek 2016)	Unfilled polyethersulfone	–	0.165	0.094	–	–
		Unfilled polyetherimide	–	0.152	0.095	–	–
		Unfilled acrylonitrile butadiene styrene copolymer	–	0.151	0.095	–	–
		Unfilled polycarbonate	–	0.153	0.095	–	–
		Acrylonitrile butadiene styrene (45%) + 150 $\mu\text{m}$ copper powder(55%)	–	0.163	0.096	–	–
		Polypropylene copolymer (15%) + iron oxide powder(75%) + impact modifier (QUEO 8210, 10%)	–	0.175	0.095	–	–
		Polyphthalamide (40%) + chopped carbon fiber (30%) + chopped glass fiber (30%)	–	0.159	0.096	–	–
		Polyphthalamide (40%) + chopped glass fiber (60%)	–	0.162	0.096	–	–
6	(Abbasova et al. 2019)	Unfilled polyphthalamide	–	0.151	0.095	–	–
		Zirconium	–	–	0.095	0.057	–
		Acrylic	–	–	0.101	0.110	–
7	(Li et al. 2017)	Composite (Ba, Al, Si)	–	–	0.117	0.084	–
		Aluminum	0.247	0.182	0.096	0.074	–
		Basalt fiber (BF) composite	0.289	0.203	0.100	0.077	–
8	(Nasehi and Ismail 2019)	Basalt fiber/erbium oxide composite	0.734	0.407	0.104	0.078	–
		Polyacrylamide/zinc oxide composite 5%	–	–	0.105	0.082	0.071
		Polyacrylamide/zinc oxide composite 10%	–	–	0.105	0.081	0.062
		Polyacrylamide/zinc oxide composite 15%	–	–	0.105	0.081	0.061
		Polyacrylamide/zinc oxide composite 20%	–	–	0.105	0.080	0.061
9	(Agar et al. 2019)	Bulk zinc oxide	–	–	0.101	0.739	0.054
		Palladium Pd/silver Ag-based alloys Pd77/Ag23	–	2.334	0.119	0.072	0.051
		Palladium Pd 75/silver Ag25	–	2.356	0.119	0.073	0.052
		Silver Ag70/palladium Pd30	–	2.402	0.123	0.074	0.051
		Palladium Pd 70/Silver Ag30	–	2.388	0.124	0.072	0.051

**Table 2** (continued)

S. n.o	Authors	Material	Mass attenuation coefficient $\mu_m$ ( $\text{cm}^2\text{g}^{-1}$ )				
			59.53 keV	80.99 keV	356.01 keV	661.66 keV	1173.25 keV
10	(Bagheri et al. 2018)	Unsaturated polyester (UP) resin 5 wt% UP/nanoclay composites,	–	–	0.100	0.074	0.033
		UP/nanoclay composites /lead oxide UPCL10,	–	–	0.120	0.078	0.032
		UP/nanoclay composites (UPCL20)	–	–	0.131	0.083	0.031
		UP/nanoclay composites (UPCL30)	–	–	0.145	0.084	0.031
		Per hydro-polysilaxane	–	0.187	–	0.081	0.059
		Poly dimethyl silaxane	–	0.189	–	0.082	0.061
		Methylsilses quioxane	–	0.179	–	0.08	0.059
11	(Belgin and Aycik 2015)	Silalkylene polymer	–	0.181	–	0.081	0.061
		Lead	0.896	0.357	–	0.100	0.056
		Isophthalic polyester (PES) based and natural mineral (hematite) HPES-10	0.258	0.242	–	0.106	0.091
		Isophthalic polyester (PES) based and natural mineral (hematite) HPES-20	0.350	0.238	–	0.112	0.084
		Isophthalic polyester (PES) based and natural mineral (hematite) HPES-30	0.423	0.321	–	0.109	0.083
		Isophthalic polyester (PES) based and natural mineral (hematite) HPES-40	0.497	0.347	–	0.098	0.092
12	(Abdo et al. 2003)	Isophthalic polyester (PES) based and natural mineral (hematite) HPES-50	0.606	0.383	–	0.098	0.083
		Fiber–plastic	–	–	–	–	0.0576
13	(Biswas et al. 2016)	Fiber–plastic–lead (FPPb) composite	–	–	–	–	0.0546
		Polyboron	–	–	–	0.086	0.065
		Pure polyethylene	–	–	–	0.088	0.067
14	(Harish et al. 2012)	Borated polyethylene	–	–	–	0.082	0.062
		Isophthalic resin (ISO) + 0% lead oxide	–	–	–	0.082	–
		Isophthalic resin (ISO) + 5% lead oxide	–	–	–	0.081	–
		Isophthalic resin (ISO) + 10% lead oxide	–	–	–	0.084	–
		Isophthalic resin (ISO) + 20% lead oxide	–	–	–	0.088	–
		Isophthalic resin (ISO) + 30% lead oxide	–	–	–	0.088	–
		Isophthalic resin (ISO) + 40% lead oxide	–	–	–	0.093	–
15	(Mahmoud et al. 2018a, b)	Isophthalic resin (ISO) + 50% lead oxide	–	–	–	0.094	–
		Raw high-density polyethylene (0% lead oxide)	0.216	0.209	0.129	0.099	0.069
		Raw high-density polyethylene-lead oxide 10% bulk lead oxide	0.685	0.406	0.144	0.100	0.070
		Raw high-density polyethylene-lead oxide 50% bulk lead oxide	3.158	1.468	0.257	0.133	0.083
		Raw high-density polyethylene-lead oxide 10% lead oxide nanoparticles	0.742	0.431	0.159	0.110	0.073
Raw high-density polyethylene-lead oxide 50% lead oxide nanoparticles	3.407	1.580	0.278	0.143	0.087		

**Table 2** (continued)

S. n.o	Authors	Material	Mass attenuation coefficient $\mu_m$ ( $\text{cm}^2\text{g}^{-1}$ )				
			59.53 keV	80.99 keV	356.01 keV	661.66 keV	1173.25 keV
16	(Alsayed et al. 2020)	High-density polyethylene	0.196	0.116	0.090	0.070	0.065
		10% High-density polyethylene /bulk zinc oxide	0.318	0.108	0.085	0.068	0.061
		20% High-density polyethylene /bulk zinc oxide	0.455	0.112	0.087	0.067	0.062
		30% High-density polyethylene /bulk zinc oxide	0.579	0.0107	0.083	0.065	0.061
		40% High-density polyethylene /bulk zinc oxide	0.703	0.111	0.083	0.065	0.061
		10% High-density polyethylene /bulk zinc oxide nano-particles	0.397	0.111	0.090	0.072	0.067
		20% High-density polyethylene /bulk zinc oxide nano-particles	0.483	0.126	0.097	0.077	0.069
		30% High-density polyethylene /bulk zinc oxide nano-particles	0.636	0.123	0.099	0.078	0.073
		40% High-density polyethylene/bulk zinc oxide nanoparticles	0.077	0.124	0.099	0.077	0.070
17	(Sheela et al. 2019)	High-density polyethylene	0.167	–	–	–	–
		High-density polyethylene + 10% Bismuth	0.609	–	–	–	–
		High-density polyethylene + 20% Bismuth	0.879	–	–	–	–
		High-density polyethylene + 40% Bismuth	2.168	–	–	–	–

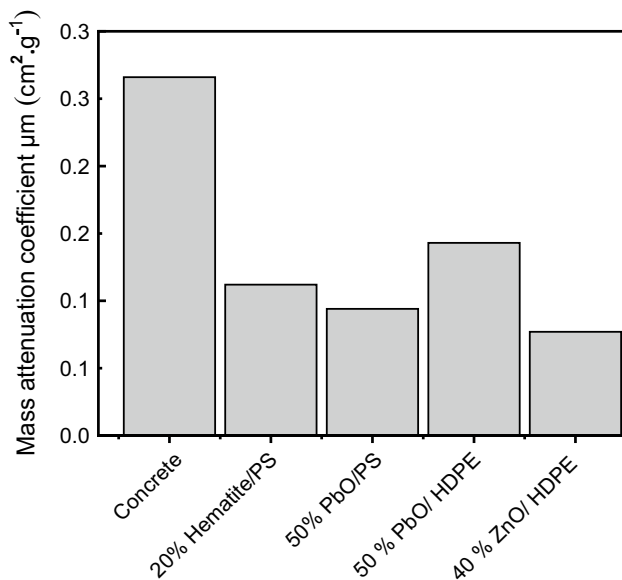


**Fig. 11** Mass attenuation coefficient of polymer nanocomposites: 20% hematite/polystyrene, 50% lead oxide/polystyrene, 50% lead oxide/high-density polyethylene, and 40% zinc oxide/high-density polyethylene compared to concrete

## Conclusion

The continuously growing demand for radiological protective materials has been discussed. The radiation shielding capabilities of a material depend on its material properties along with origin, type, energy, and exposure time of radiation, secondary radiations, and thickness of the material. The important disadvantages which limit its field of application and usage of lead and other conventionally used shielding materials have been covered. Thus, the urgent need for new radiation shielding materials is clear. Suitable to their superior properties, the polymer materials are promising candidates for mixed neutron-gamma-rays shielding. In this regard, numerous researchers have studied polymer and its composites formed by the incorporation of bulk and micro-materials. The radiation shielding abilities of such formed composite materials are increased. Nanostructure materials have recently concerned a lot of attention to scientists because of their potential applications in the development of several new technologies. One of the most applications is the radiation shielding materials which diminishes the hazard humans' dosage by interacting with gamma-ray radiations and decreasing its power.

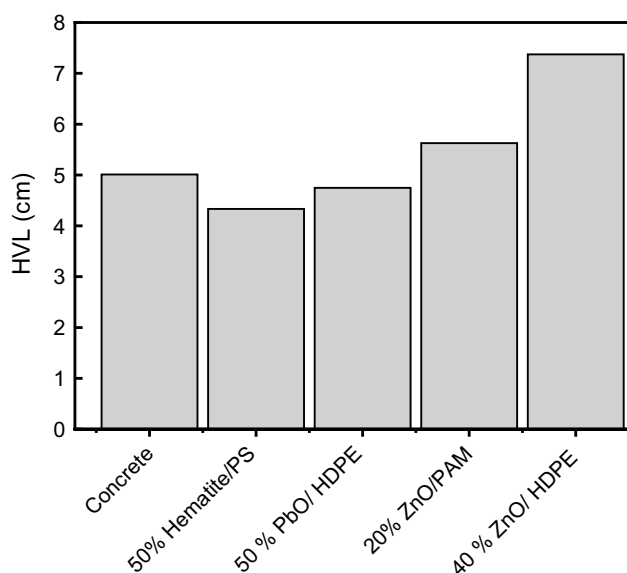


**Fig. 12** Half-value layer (HVL) measured in cm of polymer nanocomposites: 50% hematite/polystyrene, 50% lead oxide/high-density polyethylene, 20% zinc oxide /polyacrylamide (PAM), and 40% zinc oxide/high-density polyethylene compared to concrete. The characteristics of the radiation shield are used to determine their performance against gamma radiation. The incorporation of fillers into the polymer matrices improves the properties of these polymers and compensates for the drawbacks such as mechanical failure and cracks. The filler interacts with the polymer matrix by facilitating the interlocking mechanism of polymeric chains and thus increases the hardness of the composite (Rajendran et al. 2011). Also, the type, concentration, and size of filler are important parameters to be considered when synthesizing a polymer composite. The nanoparticles with their large surface-to-volume ratio are reactive fillers that can be dispersed easily within the matrix and form an interphase region between the surface of the particle and the matrix itself (Puglia and Kenny 2018)

Based on the previously published experimental results, it is clear that the polymer composites formed by the impregnation of nanomolecules are a better shield for gamma rays than the polymer itself, and the usefulness of polymer materials for neutron shielding is clear enough. Moreover, it is expected to use waste plastic materials by recycling in new

areas by obtaining novel and sustainable composites with low thickness and developed shielding properties to increase the economic feasibility and reduce the harmfulness. Recycling is the best way to manage plastic wastes since it reduces environmental impact, resource depletion, and pollution. Besides, recycling plastics consumes a smaller amount of energy when compared to energy consumption in new virgin resin production. Fundamentally, high levels of recycling, as with a reduction in use, reuse, and repair or re-manufacturing, can allow for a given level of product service with lower material input than would otherwise be required. Therefore, recycling can decrease energy and material used per unit of production and so yield improved eco-efficiency.

Several points can be summarized from the recent review article such as low atomic number polymeric materials alone which are not sufficient to attenuate/absorb highly energetic ionizing radiations such as gamma rays. One of the emerging solutions is the incorporation of other materials like high atomic number elements (other than lead), metal oxides, metal oxides, graphitic nanofibers, etc. These polymer composites have an effective low weight in comparison with a lead yet are capable shields against gamma radiation. By way of the evolution of nanotechnology, the ongoing trend is to develop novel polymer nanocomposites that would be lightweight, multifunctional, and efficient gamma-radiation shields. The world is desirous of more environmentally forthcoming materials and this has made investigators turn their attention to biodegradable or recyclable polymer nanocomposites and they have been effectively used as reinforcements in radiological protection replacing conventional materials. In this paper, a detailed review of the synthesis roots of polymer composites and their gamma-ray and neutron radiation attenuation properties has been given. This may supply an insight into polymer composites and would be useful to new researchers working in nuclear medicine, radiation therapy, nuclear industry, radiological protection, etc. The polymer matrices with some neutron absorbers impregnated by materials of the different atomic numbers are much better shielding candidates against nuclear

**Table 3** Comparison of  $\Sigma_R$  for polymers with literature

S. no.	Authors	Material	$\Sigma_R$ (cm <sup>-1</sup> )
1	(Singh and Badiger 2013)	Fly Ash Brick 1	0.0663
2	(Yılmaz et al. 2011)	Mortar mixture (MO) concrete	0.0869
3	(Lakshminarayana et al. 2020)	Bismuth tellurite and bismuth boro-tellurite (TeO <sub>2</sub> ) <sub>49</sub> (B <sub>2</sub> O <sub>3</sub> ) <sub>21</sub> (Bi <sub>2</sub> O <sub>3</sub> ) <sub>30</sub> glass	0.1080
4	(Şakar et al. 2019)	Leaded brass, Cu <sub>76</sub> Zn <sub>21</sub> P	0.1130
5	(Kaçal et al. 2019)	Polyamide-6	0.1151
6	(Sayyed 2016)	Polyethylenimine (PEI)	0.1182
7	(Elwahab et al. 2019)	High-density polyethylene + Borax (7.72%)	0.1570
8	(Elmahroug et al. 2014)	K-Resin	0.1870
9	(El Abd and Elkady 2014)	Polyethylene (PE)	0.1870

reactors, radioactive sources, collimators, etc., and these polymer composites are environmentally sound and non-toxic. Moreover, in the upcoming characterization studies such as X-ray diffraction (XRD), scanning electron microscope (SEM), energy-dispersive spectroscopy (EDAX), and Fourier transform infrared spectroscopy (FTIR) of polymer composites could be discussed later on in detail. However, further deep studies are required to get insight into radiation attenuation/absorption properties of the nanomaterials against different types of radiation.

This study has presented a reasonable review of some polymer–composite materials and their properties by introducing the importance of reusing and recycling some polymers after treatment in various applications mainly in radiation shielding against gamma rays. The addition of a certain type of fillers (metals, metal oxides, ceramics, etc.) is extremely important in enhancing the hardness, strength, and radiation absorption abilities of the synthesized composite. The future of polymer composite materials is promising, due to the extensive use of these novel materials in many fields. Emphasis on the use of recyclable and reusable polymers should be focused to reduce the harmful effects and toxicity of thermoplastics which are not degradable. Moreover, there is a need to figure out best practices to improve the properties of recyclable and reprocessed polymers to allow their use in the nuclear industry, medical diagnostics, nuclear reactors, and nuclear research organizations.

**Acknowledgements** One of the authors, Miss. Chaitali V. More, would like to thank Chhatrapati Shahu Maharaj Research Training and Human Development Institute (SARTHI), Pune (Govt. of Maharashtra, India), for the financial support under the scheme CSMNRF-2019.

**Author contributions** CVM contributed to idea for the article, literature search and data analysis, writing—original draft, writing—review and editing. ZA contributed to literature search and data analysis, writing—original draft, writing—review and editing. MSB contributed to writing—review and editing, supervision. AAT contributed to supervision. PPP contributed to supervision.

## Compliance with ethical standards

**Conflict of interest** The authors declare that they have no known competing financial interests or personal relationships that could have appeared to influence the work reported in this paper.

**Ethical approval** We confirm that this work is original and has not been published elsewhere, nor it is currently under consideration for publication elsewhere.

## References

Abbasova N, Yüksel Z, Abbasov E, Gülbiçim H, Tufan MÇ (2019) Investigation of gamma-ray attenuation parameters of some materials used in dental applications. *Results Phys* 12:2202–2205

- Abdalsalam A, Taki M, Abu Mhareb M, Alim B, Ali B, Şakar E (2020) MoO<sub>3</sub> reinforced ultra high molecular weight PE for neutrons shielding applications. *Radiat Phys Chem* 172:108852. <https://doi.org/10.1016/j.radphyschem.2020.108852>
- Abdel-Gawwad H, Mohammed M, Zakey S (2020) Preparation, performance, and stability of alkali-activated concrete waste-lead-bearing sludge composites. *J Clean Prod* 259:120924. <https://doi.org/10.1016/j.jclepro.2020.120924>
- Abdel-Haseiba A, Ahmeda Z, Hassanb MM (2018) Investigation of the gamma rays attenuation coefficients by experimental and MCNP simulation for polyamide 6/acrylonitrile-butadiene–styrene blends. *J Nucl Radiat Phys* 13(1):81–89
- Abdo AE-S, Ali M, Ismail M (2003) Natural fibre high-density polyethylene and lead oxide composites for radiation shielding. *Radiat Phys Chem* 66(3):185–195
- Adeosun SO, Lawal G, Balogun SA, Akpan EI (2012) Review of green polymer nanocomposites. *Int J Innov Res Sci Eng Technol* 11(04):385
- Adhikary KB, Pang S, Staiger MP (2008) Dimensional stability and mechanical behaviour of wood–plastic composites based on recycled and virgin high-density polyethylene (HDPE). *Compos B Eng* 39(5):807–815
- Afshar M, Morshedian J, Ahmadi S (2019) Radiation attenuation capability and flow characteristics of HDPE composite loaded with W, MoS<sub>2</sub>, and B4C. *Polym Compos* 40(1):149–158. <https://doi.org/10.1002/pc.24620>
- Agar O, Sayyed MI, Akman F, Tekin HO, Kaçal MR (2019) An extensive investigation on gamma ray shielding features of Pd/Ag-based alloys. *Nucl Eng Technol* 51(3):853–859. <https://doi.org/10.1016/j.net.2018.12.014>
- Aghaz A, Faghihi R, Mortazavi SMJ, Haghparast A, Mehdizadeh S, Sina S (2016) Radiation attenuation properties of shields containing micro and Nano WO<sub>3</sub> in diagnostic X-ray energy range. *Int J Radiat-Res* 14(2):127–131. <https://doi.org/10.18869/acadpub.ijrr.14.2.127>
- Agool IR, Kadhim KJ, Hashim A (2017) Synthesis of (PVA–PEG–PVP–ZrO<sub>2</sub>) nanocomposites for energy release and gamma shielding applications. *Int J Plast Technol* 21(2):444–453. <https://doi.org/10.1007/s12588-017-9196-1>
- Akkurt I, El-Khayatt AM (2013) Effective atomic number and electron density of marble concrete. *J Radioanal Nucl Chem*. <https://doi.org/10.1007/s10967-012-2111-5>
- Akkurt I, Kılıncarslan S, Basyigit C, Mavi B, Akyıldırım H (2009) Investigation of photon attenuation coefficient for pumice. *Int J Phys Sci* 4(10):588–591
- Akman F, Kaçal MR, Almousa N, Sayyed MI, Polat H (2020) Gamma-ray attenuation parameters for polymer composites reinforced with BaTiO<sub>3</sub> and CaWO<sub>4</sub> compounds. *Prog Nucl Energy* 121:103257. <https://doi.org/10.1016/j.pnucene.2020.103257>
- Akman F, Ogul H, Kaçal MR, Polat H, Dilsiz K, Agar O (2021) Gamma attenuation characteristics of CdTe-doped polyester composites. *Prog Nucl Energy* 131:103608. <https://doi.org/10.1016/j.pnucene.2020.103608>
- Alavian H, Tavakoli-Anbaran H (2019) Study on gamma shielding polymer composites reinforced with different sizes and proportions of tungsten particles using MCNP code. *Prog Nucl Energy* 115:91–98
- Alavian H, Tavakoli-Anbaran H (2020) Comparative study of mass attenuation coefficients for LDPE/metal oxide composites by Monte Carlo simulations. *Eur Phys J Plus* 135(1):82
- Alavian H, Samie A, Tavakoli-Anbaran H (2020) Experimental and Monte Carlo investigations of gamma ray transmission and buildup factors for inorganic nanoparticle/epoxy composites. *Radiat Phys Chem* 174:108960
- Al-Buriah MS, Singh VP, Arslan H, Awasarmol VV, Tonguc BT (2020) Gamma-ray attenuation properties of some NLO

- materials: potential use in dosimetry. *Radiat Environ Biophys* 59(1):145–150. <https://doi.org/10.1007/s00411-019-00824-y>
- Al-Dhuhaihat M, Salman M, Jubier N, Salim A (2020) Improved gamma radiation shielding traits of epoxy composites: Evaluation of mass attenuation coefficient, effective atomic and electron number. *Radiat Phys Chem* 179:109183. <https://doi.org/10.1016/j.radphyschem.2020.109183>
- Alexandre M, Dubois P (2000) Polymer-layered silicate nanocomposites: preparation, properties and uses of a new class of materials. *Mater Sci Eng R Rep* 28(1–2):1–63
- Al-Sarray E, Günoğlu K, Evcin A, Bezir N (2017) Radiation shielding properties of some composite panel. *Acta Phys Pol* 132:490–492. <https://doi.org/10.12693/APhysPolA.132.490>
- Alsayed Z, Badawi M, Awad R, Thabet A, El-Khatib A (2019) Study of some  $\gamma$ -ray attenuation parameters for new shielding materials composed of nano ZnO blended with high density polyethylene. *Nucl Technol Radiat Prot* 34:33–33. <https://doi.org/10.2298/NTRP190718033A>
- Alsayed Z, Badawi M, Awad R, Elkhatib A, Thabet A (2020) Investigation of  $\gamma$ -ray attenuation coefficients, effective atomic number and electron density for ZnO/HDPE composite. *Phys Scr*. <https://doi.org/10.1088/1402-4896/ab9a6e>
- Ambika MR, Nagaiah N, Suman SK (2017) Role of bismuth oxide as a reinforcer on gamma shielding ability of unsaturated polyester based polymer composites. *J Appl Polym Sci*. <https://doi.org/10.1002/app.44657>
- Ameen S, Akhtar MS, Shin HS (2012) Hydrazine chemical sensing by modified electrode based on in situ electrochemically synthesized polyaniline/graphene composite thin film. *Sens Actuators B Chem* 173:177–183
- ANSI/ANS (1991) Gamma-ray attenuation coefficients and buildup factor for engineering materials ANSI/ANS 6.4.3 American Nuclear Society, La Grange Park, Illinois
- Ashori A, Sheshmani S (2010) Hybrid composites made from recycled materials: moisture absorption and thickness swelling behavior. *Bioresour Technol* 101:4717–4720. <https://doi.org/10.1016/j.biortech.2010.01.060>
- Atashi P, Rahmani S, Ahadi B, Rahmati A (2018) Efficient, flexible and lead-free composite based on room temperature vulcanizing silicone rubber/W/Bi<sub>2</sub>O<sub>3</sub> for gamma ray shielding application. *J Mater Sci Mater Electron* 29:10. <https://doi.org/10.1007/s10854-018-9344-1>
- Atta E, Zakaria KM, Madbouly A (2015) Research article study on polymer clay layered nanocomposites as shielding materials for ionizing radiation. *Int J Recent Sci Res* 6(5):4263–4269
- Avella M, Errico M, Martelli S, Martuscelli E (2001) Preparation methodologies of polymer matrix nanocomposites. *Appl Organomet Chem* 5:435–439
- Awadallah-F A, Antar EM (2014) Synthesis of complexed grafted low density polyethylene films and its applicability in nuclear medicine as radiation shielding against technetium-99 m. *Polym Plast Technol Eng* 53(2):173–180. <https://doi.org/10.1080/03602559.2013.843705>
- Awaja F, Pavel D (2005) Recycling of PET. *Eur Polym J* 41:1453–1477. <https://doi.org/10.1016/j.eurpolymj.2005.02.005>
- Azadbakht B, Bagheri R (2019) Photon interaction properties of different bones from human body using MCNPX, WinXCom, XMudat, and auto-Zeff programs. *J Test Eval* 48(6):4608–4622. <https://doi.org/10.1520/JTE20180730>
- Azman NN, Siddiqui S, Hart R, Low I-M (2013) Effect of particle size, filler loadings and X-ray tube voltage on the transmitted X-ray transmission in tungsten oxide—epoxy composites. *Appl Radiat Isot* 71(1):62–67
- Bagheri K, Razavi SM, Ahmadi SJ, Kosari M, Abolghasemi H (2018) Thermal resistance, tensile properties, and gamma radiation shielding performance of unsaturated polyester/nanoclay/PbO composites. *Radiat Phys Chem* 146:5–10. <https://doi.org/10.1016/j.radphyschem.2017.12.024>
- Basfar A, Ali Z (2011) Physicochemical properties of low density polyethylene and ethylene vinyl acetate composites cross-linked by ionizing radiation. *Radiat Phys Chem* 80:257–263. <https://doi.org/10.1016/j.radphyschem.2010.07.043>
- Bedar A, Lenka RK, Goswami N, Kumar V, Debnath AK, Sen D, Kumar S, Ghodke S, Tewari PK, Bindal RC, Kar S (2019) Polysulfone-ceria mixed-matrix membrane with enhanced radiation resistance behavior. *ACS Appl Polym Mater* 1(7):1854–1865. <https://doi.org/10.1021/acsapm.9b00389>
- Bel T, Arslan C, Baydogan N (2018) Radiation shielding properties of poly(methyl methacrylate)/colemanite composite for the use in mixed irradiation fields of neutrons and gamma rays. *Mater Chem Phys*. <https://doi.org/10.1016/j.matchemphys.2018.09.014>
- Belgin EE, Aycik GA (2015) Preparation and radiation attenuation performances of metal oxide filled polyethylene based composites for ionizing electromagnetic radiation shielding applications. *J Radiational Nucl Chem* 306(1):107–117
- Berger MJ, Hubbell JH (1987) NIST standard reference database 8 (XGAM). NBSIR 87-3597, XCOM: Photon Cross Sections Database. 20899
- Berger MJ, Spencer LVC (1959) Penetration of gamma rays from isotropic sources through aluminum and concrete, US Department of Commerce, Office of Technical Services
- Bhattacharya M (2016) Polymer nanocomposites—a comparison between carbon nanotubes, graphene, and clay as nanofillers. *Materials* 9:262. <https://doi.org/10.3390/ma9040262>
- Bhosale RR, More CV, Gaikwad DK, Pawar PP, Rode MN (2017) Radiation shielding and gamma ray attenuation properties of some polymers. *Nucl Technol Radiat Prot* 32(3):288–293
- Biswas R, Sahadath H, Mollah AS, Huq MF (2016) Calculation of gamma-ray attenuation parameters for locally developed shielding material: polyboron. *J Radiat Res Appl Sci* 9(1):26–34. <https://doi.org/10.1016/j.jrras.2015.08.005>
- Blizard E, Abbott L (1962) Reactor handbook: part b: shielding, vol III. Wiley, New York
- Buyukyildiz M, Kurudirek M (2016) A study of the effective atomic number of SixPb0.7-x (Fe<sub>2</sub>O<sub>3</sub>) 0.3 ternary alloys for photons. *Nucl Technol Radiat Prot* 31(4):327–334
- Callister WD (2007) Materials science and engineering: an introduction. Wiley, New York
- Camargo PHC, Satyanarayana KG, Wypych F (2009) Nanocomposites: synthesis, structure, properties and new application opportunities. *Mater Res* 12(1):1–39
- Cao D, Yang G, Bourham M, Moneghan D (2020) Gamma radiation shielding properties of poly(methyl methacrylate)/Bi<sub>2</sub>O<sub>3</sub> composites. *Nucl Eng Technol* 52(11):2613–2619. <https://doi.org/10.1016/j.net.2020.04.026>
- Cassagnau P, Bounor-Legaré V, Fenouillot F (2007) Reactive processing of thermoplastic polymers: a review of the fundamental aspects. *Int Polym Process* 22(3):218–258. <https://doi.org/10.3139/217.2032>
- Cataldo F, Prata MJF (2019) Neutron radiation shielding with PUR composites loaded with B4C or graphite. *Fuller Nanotub Carbon Nanostruct* 27(7):531–537
- Ceh J, Youd T, Mastrovich Z, Peterson C, Khan S, Sasser TA, Sander IM, Doney J, Turner C, Leevy WM (2017) Bismuth infusion of ABS enables additive manufacturing of complex radiological phantoms and shielding equipment. *Sensors* 17(3):459
- Chai H, Tang X, Ni M, Chen F, Zhang Y, Chen D, Qiu Y (2016) Preparation and properties of novel, flexible, lead-free X-ray-shielding materials containing tungsten and bismuth(III) oxide. *J Appl Polym Sci*. <https://doi.org/10.1002/app.43012>

- Chandler H (1999) Hardness testing. ASM International, Cleveland
- Chang L, Zhang Y, Liu Y, Fang J, Luan W, Yang X, Zhang W (2015) Preparation and characterization of tungsten/epoxy composites for  $\gamma$ -rays radiation shielding. *Nucl Instrum Methods Phys Res B* 356–357:88–93. <https://doi.org/10.1016/j.nimb.2015.04.062>
- Chatterjee S, Krupadam R (2018) Amino acid-imprinted polymers as highly selective CO<sub>2</sub> capture materials. *Environ Chem Lett.* <https://doi.org/10.1007/s10311-018-0774-z>
- Chen L, Wang C, Li Q, Yang S, Hou L, Chen S (2009) In situ synthesis of transparent fluorescent ZnS–polymer nanocomposite hybrids through catalytic chain transfer polymerization technique. *J Mater Sci Mater Electron* 44(13):3413–3419
- Chiang T-C, Liu H, Tsai L, Jiang T, Ma N, Tsai F-C (2020) Improvement of the mechanical property and thermal stability of polypropylene/recycled rubber composite by chemical modification and physical blending. *Sci Rep.* <https://doi.org/10.1038/s41598-020-59191-0>
- Chinchillas-Chinchillas MJ, Gaxiola Hernández A, Alvarado C, Orozco-Carmona V, Cervantes MJ, Rodríguez-Rodríguez M, Castro-Beltrán A (2019) A new application of recycled-PET/PAN composite nanofibers to cement-based materials. *J Clean Prod* 252:119827. <https://doi.org/10.1016/j.jclepro.2019.119827>
- Cholake S, Rajarao R, Henderson P, Rajagopal R, Sahajwalla V (2017) Composite panels obtained from automotive waste plastics and agricultural macadamia shell waste. *J Clean Prod.* <https://doi.org/10.1016/j.jclepro.2017.03.074>
- Choppin G, Liljenzin J-O, Rydberg J (2002) Chapter 18. Radiation biology and radiation protection, pp 474–513
- Chowreddy RR, Nord-Varhaug K, Rapp F (2019) Recycled poly(ethylene terephthalate)/clay nanocomposites: rheology, thermal and mechanical properties. *J Polym Environ* 27(1):37–49
- Daima H, Shankar S, Anderson A, Selvakannan PR, Bhargava S, Bansal V (2018) Complexation of plasmid DNA and poly(ethylene oxide)/poly(propylene oxide) polymers for safe gene delivery. *Environ Chem Lett.* <https://doi.org/10.1007/s10311-018-0756-1>
- Das NC, Liu Y, Yang K, Peng W, Maiti S, Wang H (2009) Single-walled carbon nanotube/poly (methyl methacrylate) composites for electromagnetic interference shielding. *Polym Eng Sci* 49(8):1627–1634
- Dehghani A, Ardekani SM, Al-Maadeed MA, Hassan A, Wahit MU (2013) Mechanical and thermal properties of date palm leaf fiber reinforced recycled poly(ethylene terephthalate) composites. *Mater Des* 52:841–848
- Demir İ, Gümüş M, Gökçe HS (2020) Gamma ray and neutron shielding characteristics of polypropylene fiber-reinforced heavyweight concrete exposed to high temperatures. *Constr Build Mater* 257:119596. <https://doi.org/10.1016/j.conbuildmat.2020.119596>
- El Abd AA, Elkady AS (2014) A method for simultaneous determination of effective removal cross-section for fast neutrons and mass absorption coefficient for gamma rays. *Mater Sci Eng* 2(2):1–6
- El-Fiki S, El Kameesy SU, Nashar DE, Abou-Leila MA, El-Mansy MK, Ahmed M (2015) Influence of bismuth contents on mechanical and gamma ray attenuation properties of silicone rubber composite. *Int J Adv Res* 3(6):1035–1041
- El-Khatib AM, Abbas MI, Elzaher MA, Badawi MS, Alabsy MT, Alharshan GA, Aloraini DA (2019) Gamma attenuation coefficients of nano cadmium oxide/high density polyethylene composites. *Sci Rep* 9(1):16012. <https://doi.org/10.1038/s41598-019-52220-7>
- El-Khayatt A (2010) Calculation of fast neutron removal cross-sections for some compounds and materials. *Ann Nucl Energy* 37:218–222. <https://doi.org/10.1016/j.anucene.2009.10.022>
- El-Khayatt AM (2011) NXcom—a program for calculating attenuation coefficients of fast neutrons and gamma-rays. *Ann Nucl Energy* 38(1):128–132
- El-Khayatt AM, Abdo AE-S (2009) MERCFSF-N: a program for the calculation of fast neutron removal cross sections in composite shields. *Ann Nucl Energy* 36(6):832–836
- Elmahroug Y, Tellili B, Souga C (2014) Determination of shielding parameters for different types of resins. *Ann Nucl Energy* 63:619–623. <https://doi.org/10.1016/j.anucene.2013.09.007>
- El-Mekkawi D, Abdelwahab NA, Mohamed W, Taha N, Abdel-Mottaleb M (2019) Solar photocatalytic treatment of industrial wastewater utilizing recycled polymeric disposals as TiO<sub>2</sub> supports. *J Clean Prod* 249:119430. <https://doi.org/10.1016/j.jclepro.2019.119430>
- Elwahab N, Helal N, Mohamed T, Shahin F, Ali F (2019) New shielding composite paste for mixed fields of fast neutrons and gamma rays. *Mater Chem Phys.* <https://doi.org/10.1016/j.matchemphys.2019.05.059>
- Evenc O, Evenc A, Bezir N, Günoğlu K, Ersoy B (2017) Production of barite and boroncarbide doped radiation shielding polymer composite panels. *Acta Phys Pol* 132:1145–1148. <https://doi.org/10.12693/APhysPolA.132.1145>
- Fontainha CCP, Baptista Neto AT, Santos AP, Faria LOD (2016) P (VDF-TrFE)/ZrO<sub>2</sub> polymer-composites for x-ray shielding. *Mater Res* 19(2):426–433
- Gaikwad K, Singh S, Aji A (2018) Moisture absorbers for food packaging applications. *Environ Chem Lett.* <https://doi.org/10.1007/s10311-018-0810-z>
- Galante A, Campos L (2010) Characterization of polycarbonate dosimeter for gamma-radiation dosimetry. In: Proceedings of third European IPRA congress, Helsinki, Finland
- Gerward L, Guilbert N, Jensen KB, Levring H (2004) WinXCom—a program for calculating X-ray attenuation coefficients. *Radiat Phys Chem* 71(3):653–654. <https://doi.org/10.1016/j.radphyschem.2004.04.040>
- Glasstone S, Sesonske A (2012) Nuclear reactor engineering: reactor systems engineering. Springer, New York
- Grégorio C, Torri G, Lichtfouse E, Kyzas G, Wilson L, Crini N (2019) Dye removal by biosorption using cross-linked chitosan-based hydrogels. *Environ Chem Lett.* <https://doi.org/10.1007/s10311-019-00903-y>
- Grigoriadou I, Paraskevopoulos K, Chrissafis K, Pavlidou E, Stamkopoulos T-G, Bikiaris D (2011) Effect of different nanoparticles on HDPE UV stability. *Polym Degrad Stab* 96:151–163. <https://doi.org/10.1016/j.polymdegradstab.2010.10.001>
- Gryczak M, Wong J, Thiemann C, Ferrari B, Werner I, Petzhold C (2020) Recycled low-density polyethylene composite to mitigate the environmental impacts generated from coal mining waste in Brazil. *J Environ Manag* 260:110149. <https://doi.org/10.1016/j.jenvman.2020.110149>
- Gu S, Kang X, Wang L, Lichtfouse E, Wang C (2018) Clay mineral adsorbents for heavy metal removal from wastewater: a review. *Environ Chem Lett.* <https://doi.org/10.1007/s10311-018-0813-9>
- Gudadhe A, Bachhar N, Kumar A, Andrade P, Kumaraswamy G (2019) Three-dimensional printing with waste high-density polyethylene. *ACS Appl Polym Mater* 1(11):3157–3164. <https://doi.org/10.1021/acsapm.9b00813>
- Gupta AK, Biswal M, Mohanty S, Nayak S (2014) Mechanical and thermal degradation behavior of sisal fiber (SF) reinforced recycled polypropylene (RPP) composites. *Fibers Polym* 15(5):994–1003
- Gurler O, Akar Tarim U (2016) Determination of radiation shielding properties of some polymer and plastic materials against gamma-rays. *Acta Phys Pol* 130:236–238. <https://doi.org/10.12693/APhysPolA.130.236>
- Gwailly SE (2002) Galena/(NR+SBR) rubber composites as gamma radiation shields. *Polym Test* 21(8):883–887
- Hager IZ, Rammah YS, Othman HA, Ibrahim EM, Hassan SF, Sallam FH (2019) Nano-structured natural bentonite clay coated

- by polyvinyl alcohol polymer for gamma rays attenuation. *J Theor Appl Phys* 13(2):141–153. <https://doi.org/10.1007/s40094-019-0332-5>
- Hamim F, Ghani S, Zainuddin F (2016) Properties of recycled high density polyethylene (RHDPE)/ethylene vinyl acetate (EVA) blends: the effect of blends composition and compatibilisers. *J Phys Sci* 27:23–39. <https://doi.org/10.21315/jps2016.27.2.3>
- Harima Y (1983) An approximation of gamma-ray buildup factors by modified geometrical progression. *Nucl Sci Eng (US)* 83:2. <https://doi.org/10.13182/NSE83-A18222>
- Harish V, Nagaiah N, Kumar HG (2012) Lead oxides filled isophthalic resin polymer composites for gamma radiation shielding applications. *Indian J Pure Appl Phys* 50:847–850
- Harrison C, Burgett E, Hertel N, Grulke E (2008) Polyethylene/boron composites for radiation shielding applications. *AIP Conf Proc* 969(1):484–491. <https://doi.org/10.1063/1.2845006>
- Hassan H, Badran H, Aydarous A, Sharshar T (2015) Studying the effect of nano lead compounds additives on the concrete shielding properties for  $\gamma$ -rays. *Nucl Instrum Methods Phys Res B* 360:81–89
- Hebbar R, Isloor A, Inamuddin I, Asiri AM (2017) Carbon nanotube- and graphene-based advanced membrane materials for desalination. *Environ Chem Lett.* <https://doi.org/10.1007/s10311-017-0653-z>
- Hellström K, Dioszegi A, Diaconu L (2017) A broad literature review of density measurements of liquid cast iron. *Metals.* <https://doi.org/10.3390/met7050165>
- Hopewell J, Dvorak R, Kosior E (2009) Plastics recycling: challenges and opportunities. *Philos Trans R Soc Lond B Biol Sci* 364:2115–2126. <https://doi.org/10.1098/rstb.2008.0311>
- Hussain R, Haq ZU, Mohammad D (1997) A study of the shielding properties of poly ethylene glycol-lead oxide composite. *J Islamic Acad Sci* 10(3):81–84
- Inacio AL, Nonato RC, Bonse BC (2017) Recycled PP/EPDM/talc reinforced with bamboo fiber: assessment of fiber and compatibilizer content on properties using factorial design. *Polym Test* 61:214–222
- Issa SAM, Mostafa AMA, Hanafy TA, Dong M, Xue X (2019) Comparison study of photon attenuation characteristics of Poly vinyl alcohol (PVA) doped with  $Pb(NO_3)_2$  by MCNP5 code, XCOM and experimental results. *Prog Nucl Energy* 111:15–23. <https://doi.org/10.1016/j.pnucene.2018.10.018>
- Jumpee C, Wongsawaeng D (2015) Innovative neutron shielding materials composed of natural rubber-styrene butadiene rubber blends, boron oxide and iron (III) oxide. *J Phys Conf Ser* 611:012019
- Kaçal M, Akman F, Sayyed M (2019) Evaluation of gamma-ray and neutron attenuation properties of some polymers. *Nucl Eng Technol* 51(3):818–824
- Kaçal MR, Polat H, Oltulu M, Akman F, Agar O, Tekin HO (2020) Gamma shielding and compressive strength analyses of polyester composites reinforced with zinc: an experiment, theoretical, and simulation based study. *Appl Phys A* 126(3):205. <https://doi.org/10.1007/s00339-020-3382-2>
- Kaçal MR, Dilsiz K, Akman F, Polat H (2021) Analysis of radiation attenuation properties for Polyester/ $Li_2WO_4$  composites. *Radiat Phys Chem* 179:109257. <https://doi.org/10.1016/j.radphyschem.2020.109257>
- Kaloshkin S, Tcherdyntsev V, Gorshenkov M, Gulbin V, Kuznetsov S (2012) Radiation-protective polymer-matrix nanostructured composites. *J Alloys Compd* 536:S522–S526
- Kaphle A, Umaphathi NPNA, Daima H (2017) Nanomaterials for agriculture, food and environment: applications, toxicity and regulation. *Environ Chem Lett.* <https://doi.org/10.1007/s10311-017-0662-y>
- Kaushik A, Singh M, Verma G (2010) Green nanocomposites based on thermoplastic starch and steam exploded cellulose nanofibrils from wheat straw. *Carbohydr Polym* 82:337–345. <https://doi.org/10.1016/j.carbpol.2010.04.063>
- Kazemi F, Malekie S, Hosseini MA (2019) A Monte Carlo study on the shielding properties of a novel polyvinyl alcohol (PVA)/ $WO_3$  composite, against gamma rays, using the MCNPX code. *J Biomed Phys Eng* 9(4):465–472. <https://doi.org/10.31661/jbpe.v0i0.1114>
- Kilicoglu O, Kara U, Inanc I (2021) The impact of polymer additive for N95 masks on gamma-ray attenuation properties. *Mater Chem Phys* 260:124093. <https://doi.org/10.1016/j.matchemphys.2020.124093>
- Kráčalík M, Pospíšil L, Šlouf M, Mikešová J, Sikora A, Šimoník J, Fortelný I (2008) Effect of glass fibers on rheology, thermal and mechanical properties of recycled PET. *Polym Compos* 29(8):915–921
- Kumar A (2017) Gamma ray shielding properties of  $PbO-Li_2O-B_2O_3$  glasses. *Radiat Phys Chem* 136:50–53. <https://doi.org/10.1016/j.radphyschem.2017.03.023>
- Kumar AP, Depan D, Singh Tomer N, Singh RP (2009) Nanoscale particles for polymer degradation and stabilization—trends and future perspectives. *Prog Polym Sci* 34(6):479–515. <https://doi.org/10.1016/j.progpolymsci.2009.01.002>
- Kumar S, Raju S, Mohana N, Sampath PS, Jayakumari LS (2014) effects of nanomaterials on polymer composites—an expatiated view. *Rev Adv Mater Sci* 38(1):40–54
- Lakshminarayana G, Kebaili I, Dong M, Al-Buriah M, Dahshan A, Kityk I, Lee D-E, Yoon J, Park T (2020) Estimation of gamma-rays, and fast and the thermal neutrons attenuation characteristics for bismuth tellurite and bismuth boro-tellurite glass systems. *J Mater Sci Mater Electron* 55(14):5750–5771
- Lee K-H, Noh N-S, Shin D-H, Seo Y (2002) Comparison of plastic types for catalytic degradation of waste plastics into liquid product with spent FCC catalyst. *Polym Degrad Stab* 78:539–544. [https://doi.org/10.1016/S0141-3910\(02\)00227-6](https://doi.org/10.1016/S0141-3910(02)00227-6)
- Lee S, Kang I-A, Doh G-H, Yoon H, Park B-D, Wu Q (2008) Thermal and mechanical properties of wood flour/talc-filled polylactic acid composites: effect of filler content and coupling treatment. *J Thermoplast Compos Mater* 21:209–223. <https://doi.org/10.1177/0892705708089473>
- Levet A, Kavaz E, Özdemir Y (2020) An experimental study on the investigation of nuclear radiation shielding characteristics in iron-boron alloys. *J Alloys Compd* 819:152946. <https://doi.org/10.1016/j.jallcom.2019.152946>
- Li R, Gu Y, Wang Y, Yang Z, Li M, Zhang Z (2017) Effect of particle size on gamma radiation shielding property of gadolinium oxide dispersed epoxy resin matrix composite. *Mater Res Express* 4(3):035035
- Li Q, Wei Q, Zheng W, Zheng Y, Okosi N, Wang Z, Su M (2018) Enhanced radiation shielding with conformal light-weight nanoparticle-polymer composite. *ACS Appl Mater Interfaces* 10(41):35510–35515
- Lichtfouse E, Crini N, Fourmentin M, Zemmouri H, Queiroz L, Mohd Tadza MY, Picos Corrales L, Pei H, Wilson L, C. grégorio, (2019) Chitosan for direct bioflocculation of wastewater. *Environ Chem Lett* 17:10. <https://doi.org/10.1007/s10311-019-00900-1>
- Liikanen M, Grönman K, Deviatkin I, Havukainen J, Hyvärinen M, Kärki T, Varis J, Soukka R, Horttanainen M (2019) Construction and demolition waste as a raw material for wood polymer composites—assessment of environmental impacts. *J Clean Prod* 225:716–727
- Liu K, Piggott MR (1995) Shear strength of polymers and fibre composites: 1. thermoplastic and thermoset polymers. *Composites* 26:829–840. [https://doi.org/10.1016/0010-4361\(95\)90876-2](https://doi.org/10.1016/0010-4361(95)90876-2)

- Lopes J, Martins M, Nogueira H, Estrada A, Trindade T (2021) Carbon-based heterogeneous photocatalysts for water cleaning technologies: a review. *Environ Chem Lett.* <https://doi.org/10.1007/s10311-020-01092-9>
- Luković J, Babić B, Bučević D, Prekajski M, Pantić J, Baščarević Z, Matović B (2015) Synthesis and characterization of tungsten carbide fine powders. *Ceram Int* 41(1):1271–1277. <https://doi.org/10.1016/j.ceramint.2014.09.057>
- Ma J, Qin G, Zhang Y, Sun J, Wang S, Jiang L (2018) Heavy metal removal from aqueous solutions by calcium silicate powder from waste coal fly-ash. *J Clean Prod* 182:776–782
- Ma Z, Guo W, Yang R (2020) Performance evaluation of the polyurethane-based composites prepared with recycled polymer concrete aggregate. *Materials* 13:616. <https://doi.org/10.3390/ma13030616>
- Mahmoud ME, El-Khatib AM, Badawi MS, Rashad AR, El-Sharkawy RM, Thabet AA (2018a) Fabrication, characterization and gamma rays shielding properties of nano and micro lead oxide-dispersed-high density polyethylene composites. *Radiat Phys Chem* 145:160–173. <https://doi.org/10.1016/j.radphyschem.2017.10.017>
- Mahmoud ME, El-Khatib AM, Badawi MS, Rashad AR, El-Sharkawy RM, Thabet AA (2018b) Recycled high-density polyethylene plastics added with lead oxide nanoparticles as sustainable radiation shielding materials. *J Clean Prod* 176:276–287. <https://doi.org/10.1016/j.jclepro.2017.12.100>
- Maity K, Garain S, Henkel K, Schmeißer D, Mandal D (2020) Self-powered human-health monitoring through aligned pvdF nanofibers interfaced skin-interactive piezoelectric sensor. *ACS Appl Polym Mater* 2(2):862–878. <https://doi.org/10.1021/acsapm.9b00846>
- Makvandi P, Iftekhar S, Pizzetti F, Zarepour A, Nazarzadeh Zare E, Ashrafizadeh M, Agarwal T, Padil V, Mohammadinejad R, Silanpää M, Perale G, Zarrabi A, Rossi F (2020) Functionalization of polymers and nanomaterials for water treatment, food packaging, textile and biomedical applications: a review. *Environ. Chem. Lett.* <https://doi.org/10.1007/s10311-020-01089-4>
- Mani V, Prasad N, Kelkar A (2016) Ultra high molecular weight polyethylene (UHMWPE) fiber epoxy composite hybridized with nanoparticles of gadolinium and boron for radiation shielding. In: SPIE optical engineering and applications, proceedings planetary defense and space environment applications
- Manjunatha HC (2017) A study of gamma attenuation parameters in poly methyl methacrylate and Kapton. *Radiat Phys Chem* 137:254–259. <https://doi.org/10.1016/j.radphyschem.2016.01.024>
- Mann K, Rani A, Heer M (2015a) Shielding behaviors of some polymer and plastic materials for gamma-rays. *Radiat Phys Chem* 106:247–254. <https://doi.org/10.1016/j.radphyschem.2014.08.005>
- Mann KS, Rani A, Heer MS (2015b) Shielding behaviors of some polymer and plastic materials for gamma-rays. *Radiat Phys Chem* 106:247–254. <https://doi.org/10.1016/j.radphyschem.2014.08.005>
- Mann HS, Brar GS, Mudahar GS (2016) Gamma-ray shielding effectiveness of novel light-weight clay-flyash bricks. *Radiat Phys Chem* 127:97–101. <https://doi.org/10.1016/j.radphyschem.2016.06.013>
- Mao X, Wang L, Gu S, Duan Y, Zhu Y, Wang C, Lichtfouse E (2018) Synthesis of a three-dimensional network sodium alginate-poly(acrylic acid)/attapulgite hydrogel with good mechanic property and reusability for efficient adsorption of  $\text{Cu}^{2+}$  and  $\text{Pb}^{2+}$ . *Environ Chem Lett.* <https://doi.org/10.1007/s10311-018-0708-9>
- Marcelo LR, de Gois JS, da Silva AA, Cesar DV (2020) Synthesis of iron-based magnetic nanocomposites and applications in adsorption processes for water treatment: a review. *Environ Chem Lett.* <https://doi.org/10.1007/s10311-020-01134-2>
- Marinkovic A, Radoman T, Dzunuzovic ES, Branko B, Balanc B, Spasojevic P (2013) Mechanical properties of composites based on unsaturated polyester resins obtained by chemical recycling of poly (ethylene terephthalate). *Hem Ind* 67(6):913–922
- McMillan J (2019) Radiation shielding composites using thermoplastic polymers mouldable at low temperature. *Phys Instrum Detect*
- Mirji R, Lobo B (2017a) Computation of the mass attenuation coefficient of polymeric materials at specific gamma photon energies. *Radiat Phys Chem* 135:32–44. <https://doi.org/10.1016/j.radphyschem.2017.03.001>
- Mirji R, Lobo B (2017) Radiation shielding materials: a brief review on methods, scope and significance
- Mirji R, Lobo B (2020) Study of polycarbonate–bismuth nitrate composite for shielding against gamma radiation. *J Radioanal Nucl Chem* 324(1):7–19. <https://doi.org/10.1007/s10967-020-07038-3>
- Miskolczi N, Prof L, Bartha GD, Jóver B (2004) Thermal degradation of municipal plastic waste for production of fuel-like hydrocarbons. *Polym Degrad Stab* 86:357–366. <https://doi.org/10.1016/j.polymdegradstab.2004.04.025>
- More CV, Lokhande RM, Pawar PP (2016) Effective atomic number and electron density of amino acids within the energy range of 0.122–1.330 MeV. *Radiat Phys Chem* 125:14–20
- More CV, Bhosale RR, Pawar PP (2017) Detection of new polymer materials as gamma-ray-shielding materials. *Radiat Eff Defects Solids* 172(5–6):469–484. <https://doi.org/10.1080/10420150.2017.1336765>
- More CV, Alavian H, Pawar PP (2020) Evaluation of gamma-ray attenuation characteristics of some thermoplastic polymers: Experimental, WinXCom and MCNPX studies. *J Non-Cryst Solids* 546:120277. <https://doi.org/10.1016/j.jnoncrystol.2020.120277>
- More CV, Pawar PP, Badawi MS, Thabet AA (2020) Extensive theoretical study of gamma-ray shielding parameters using epoxy resin-metal chloride mixtures. *Nucl Technol Radiat Prot* 35(2):138–149
- Mostafa AMA, Issa SAM, Sayyed MI (2017) Gamma ray shielding properties of  $\text{PbO-B}_2\text{O}_3\text{-P}_2\text{O}_5$  doped with  $\text{WO}_3$ . *J Alloys Compd* 708:294–300. <https://doi.org/10.1016/j.jallcom.2017.02.303>
- Mulenon George M, Liu J, Lujan H, Guo B, Lichtfouse E, Sharma V, Sayes C (2020) Copper, silver, and titania nanoparticles do not release ions under anoxic conditions and release only minute ion levels under oxic conditions in water: evidence for the low toxicity of nanoparticles. *Environ Chem Lett.* <https://doi.org/10.1007/s10311-020-00985-z>
- Muthamma MV, Bubbly SG, Gudennavar SB, Narendranath KCS (2019) Poly(vinyl alcohol)-bismuth oxide composites for X-ray and  $\gamma$ -ray shielding applications. *J Appl Polym Sci* 136(37):47949. <https://doi.org/10.1002/app.47949>
- Nagaraja N, Manjunatha H, Seenappa L, Sridhar K, Ramalingam H (2020) Radiation shielding properties of silicon polymers. *Radiat Phys Chem* 171:108723
- Nanda S, Berruti F (2020) Thermochemical conversion of plastic waste to fuels: a review. *Environ Chem Lett.* <https://doi.org/10.1007/s10311-020-01094-7>
- Nasehi F, Ismail M (2019) Evaluation of X and gamma-rays attenuation parameters for polyacrylamide and ZnO composites as light shielding materials using MCNP and X-COM simulation. *Nucl Med Radiat Ther* 10(404):2
- Nguyen M, Vu T, Nguyen T, Nguyen T, Ha Thuc N, Bui Q-B, Colin J, Perre P (2020) Synergistic influences of stearic acid coating and recycled PET microfibers on the enhanced properties of composite materials. *Materials* 13:1461. <https://doi.org/10.3390/ma13061461>
- Ninyong K, Wimolmala E, Sombatsomporn N, Saenboonruang K (2019) Properties of natural rubber (NR) and wood/NR composites

- as gamma shielding materials. *IOP Conf Ser Mater Sci Eng* 526:012038. <https://doi.org/10.1088/1757-899x/526/1/012038>
- Njuguna J, Pielichowski K, Alcock JR (2007) Epoxy-based fibre reinforced nanocomposites. *Adv Eng Mater* 9(10):835–847
- Okamoto M (2003) Biodegradable polymer/layered silicate nanocomposites. In: *Handbook of biodegradable polymeric materials and their applications*, pp 153–197
- Olivera S, Chaitra K, Venkatesh K, Muralidhara H, Inamuddin I, Asiri AM, Ahamed M (2018) Cerium dioxide and composites for the removal of toxic metal ions. *Environ Chem Lett*. <https://doi.org/10.1007/s10311-018-0747-2>
- Osman A, Abdel-Monem A, Mansour Aly F (2015) Investigation the shielding properties of alumina reinforced composites. *J Chem Bio Phys Sci Sec C* 6:302–315
- Oto B, Yıldız N, Akdemir F, Kavaz E (2015) Investigation of gamma radiation shielding properties of various ores. *Prog Nucl Energy* 85:391–403. <https://doi.org/10.1016/j.pnucene.2015.07.016>
- Özdemir T, Güngör A, Akbay I, Uzun H, Babuçcuoglu Y (2018) Nano lead oxide and epdm composite for development of polymer based radiation shielding material: gamma irradiation and attenuation tests. *Radiat Phys Chem* 144:248–255
- Padervand M, Lichtfouse E, Robert D, Wang C (2020) Removal of microplastics from the environment: a review. *Environ Chem Lett*. <https://doi.org/10.1007/s10311-020-00983-1>
- Parhi R (2020) Drug delivery applications of chitin and chitosan: a review. *Environ Chem Lett*. <https://doi.org/10.1007/s10311-020-00963-5>
- Pascoe RD (2003) Sorting of waste plastics for recycling. an introduction to automotive composites. K. L. Nick Tucker Rapra Technol Ltd 24:49–49
- Pavlenko V, Cherkashina N, Yastrebinsky R (2019) Synthesis and radiation shielding properties of polyimide/Bi<sub>2</sub>O<sub>3</sub> composites. *Heliyon* 5(5):e01703
- Phong NT, Gabr MH, Okubo K, Chuong B, Fujii T (2013) Enhancement of mechanical properties of carbon fabric/epoxy composites using micro/nano-sized bamboo fibrils. *Mater Des* 47:624–632. <https://doi.org/10.1016/j.matdes.2012.12.057>
- Plionis AA, Garcia SR, Gonzales ER, Porterfield DR, Peterson DS (2009) Replacement of lead bricks with non-hazardous polymer-bismuth for low-energy gamma shielding. *J Radioanal Nucl Chem* 282(1):239. <https://doi.org/10.1007/s10967-009-0245-x>
- Puglia D, Kenny J (2018) Structure-property relationships of thermoset nanocomposites. In: *Thermosets (second edition) structure, properties, and applications*. Elsevier, pp 231–276
- Qasim U, Ahmed A, Osman AA, Al-Muhtaseb A, Farrell C, Al-Abri M, Muzaffar R, Vo D-V, Vo N, Farrukh D, Rooney W (2020) Renewable cellulosic nanocomposites for food packaging to avoid fossil fuel plastic pollution: a review. *Environ Chem Lett*. <https://doi.org/10.1007/s10311-020-01090-x>
- Qu P, Gao Y, Wu GF, Zhang LP (2010) Nanocomposites of Poly(lactic acid) reinforced with cellulose nanofibrils. *BioResources* 5:1811–1823
- Rai M, Ingle A, Gupta I, Pandit R, Paralikar P, Gade A, Chaud M, Santos C (2018) Smart nanopackaging for the enhancement of food shelf life. *Environ Chem Lett*. <https://doi.org/10.1007/s10311-018-0794-8>
- Rajendran B, Muthusamy S, Tos VC (2011) Mechanical and thermal properties of unsaturated polyester/calcium carbonate nanocomposites. *J Reinf Plast Compos* 30(18):1549–1556
- Ramli RA, Zakaria NZ, Rahman UUA, Bakhtiar NBA, Mustapha SNH, Lian YM (2018) Effect of mineral fillers on mechanical, thermal and morphological properties of kenaf recycled polyethylene wood plastic composite. *Eur J Wood Products* 76(6):1737–1743
- Rani N, Vermani YK, Singh T (2020) Gamma radiation shielding properties of some Bi-Sn-Zn alloys. *J Radiol Prot* 40(1):296–310. <https://doi.org/10.1088/1361-6498/ab6aaf>
- Rathi B, Ponnusamy SK (2020) Electrodeionization theory, mechanism and environmental applications: a review. *Environ Chem Lett*. <https://doi.org/10.1007/s10311-020-01006-9>
- Rusmirović J, Trifkovic K, Bugarski B, Pavlović VB, Džunuzović J, Tomić M, Marinković AD (2016) High performance unsaturated polyester based nanocomposites: effect of vinyl modified nanosilica on mechanical properties. *Express Polym Lett* 10(2):139–159
- Saiyad DM, Devashrayee N, Mewada R (2014) Study the effect of dispersion of filler in polymer composite for radiation shielding. *Polym Compos*. <https://doi.org/10.1002/pc.22776>
- Şakar E, Büyükyıldız M, Alım B, Şakar BC, Kurudirek M (2019) Lead brass alloys for gamma-ray shielding applications. *Radiat Phys Chem* 159:64–69
- Salipira K, Mamba B, Krause R, Malefetse T, Durbach S (2007) Carbon nanotubes and cyclodextrin polymers for removing organic pollutants from water. *Environ Chem Lett* 5:13–17. <https://doi.org/10.1007/s10311-006-0057-y>
- Sanjay M, Arpitha G, Laxmana Naik L, Gopalakrishna K, Yogesh B (2016) Studies on mechanical properties of banana/e-glass fabrics reinforced polyester hybrid composites. *J Mater Environ Sci* 7(9):3179–3192
- Sathiyaraj S, Samuel JJ, Valeriano C, Kurudirek M (2017) Effective atomic number and buildup factor calculations for metal nano particle doped polymer gel. *Vacuum*. <https://doi.org/10.1016/j.vacuum.2017.06.005>
- Sayyed MI (2016) Investigation of shielding parameters for smart polymers. *Chin J Phys* 54(3):408–415. <https://doi.org/10.1016/j.cjph.2016.05.002>
- Sayyed MI, Lakshminarayana G, Kityk IV, Mahdi MA (2017) Evaluation of shielding parameters for heavy metal fluoride based tellurite-rich glasses for gamma ray shielding applications. *Radiat Phys Chem* 139:33–39. <https://doi.org/10.1016/j.radphyschem.2017.05.013>
- Sayyed M, Lakshminarayana G, Mahdi M (2017) Evaluation of radiation shielding parameters for optical materials. *Chalcogenide Lett* 14(2):43–47
- Sayyed MI, El-Mesady IA, Abouhaswa AS, Askin A, Rammah YS (2019) Comprehensive study on the structural, optical, physical and gamma photon shielding features of B<sub>2</sub>O<sub>3</sub>-Bi<sub>2</sub>O<sub>3</sub>-PbO-TiO<sub>2</sub> glasses using WinXCOM and Geant4 code. *J Mol Struct* 1197:656–665. <https://doi.org/10.1016/j.molstruc.2019.07.100>
- Sharma G, Thakur B, Naushad M, Kumar A, Stadler FJ, Alfadul SM, Mola GT (2018) Applications of nanocomposite hydrogels for biomedical engineering and environmental protection. *Environ Chem Lett* 16(1):113–146. <https://doi.org/10.1007/s10311-017-0671-x>
- Sharma A, Singh B, Sandhu BS (2019) Investigation of photon interaction parameters of polymeric materials using Monte Carlo simulation. *Chin J Phys* 60:709–719. <https://doi.org/10.1016/j.cjph.2019.06.011>
- Sharma A, Sayyed MI, Agar O, Kaçal MR, Polat H, Akman F (2020) Photon-shielding performance of bismuth oxychloride-filled polyester concretes. *Mater Chem Phys* 241:122330. <https://doi.org/10.1016/j.matchemphys.2019.122330>
- Sheela M, Kamat VA, Kiran K, Eshwarappa K (2019) Preparation and characterization of bismuth-filled high-density polyethylene composites for gamma-ray shielding. *Radiat Protect Environ* 42(4):180
- Shent H, Pugh R, Forsberg E (1999) A review of plastics waste recycling and the flotation of plastics. *Resour Conserv Recycl* 25:85–109. [https://doi.org/10.1016/S0921-3449\(98\)00017-2](https://doi.org/10.1016/S0921-3449(98)00017-2)

- Shi G, He LJ, Chen CZ, Liu JF, Liu QZ, Chen HY (2011) A novel nanocomposite based on recycled poly (ethylene terephthalate)/ABS blends and nano-SiO<sub>2</sub>. *Adv Mater Res Trans Tech Publ*
- Shik NA, Gholamzadeh L (2018) X-ray shielding performance of the EPVC composites with micro-or nanoparticles of WO<sub>3</sub>, PbO or Bi<sub>2</sub>O<sub>3</sub>. *Appl Radiat Isot* 139:61–65
- Siddiqui MTH, Nizamuddin S, Baloch HA, Mubarak NM, Dumbre DK, Inamuddin AM, Asiri AW, Bhutto MS, Griffin GJ (2018) Synthesis of magnetic carbon nanocomposites by hydrothermal carbonization and pyrolysis. *Environ Chem Lett* 16(3):821–844. <https://doi.org/10.1007/s10311-018-0724-9>
- Singh VP, Badiger N (2013) A comprehensive study on gamma-ray exposure build-up factors and fast neutron removal cross sections of fly-ash bricks. *J Ceram* 2013:1–13
- Singh VP, Badiger NM, Kaewkhao J (2014) Radiation shielding competence of silicate and borate heavy metal oxide glasses: Comparative study. *J Non-Cryst Solids* 404:167–173. <https://doi.org/10.1016/j.jnoncrsol.2014.08.003>
- Singh VP, Badiger NM, Chanthima N, Kaewkhao J (2014) Evaluation of gamma-ray exposure buildup factors and neutron shielding for bismuth borosilicate glasses. *Radiat Phys Chem* 98:14–21. <https://doi.org/10.1016/j.radphyschem.2013.12.029>
- Singh VP, Shirmardi SP, Medhat ME, Badiger NM (2015) Determination of mass attenuation coefficient for some polymers using Monte Carlo simulation. *Vacuum* 119:284–288. <https://doi.org/10.1016/j.vacuum.2015.06.006>
- Song R, Murphy M, Li C, Ting K, Soo C, Zheng Z (2018) Current development of biodegradable polymeric materials for biomedical applications. *Drug Des Dev Ther* 12:3117–3145. <https://doi.org/10.2147/DDDT.S165440>
- Sorrentino A, Gorrasi G, Lichtfouse E (2020) Back to plastic pollution in COVID times. *Environ Chem Lett*. <https://doi.org/10.1007/s10311-020-01129-z>
- Soundharraj P, Dhinasekaran D, Lichtfouse E (2020) Plant-derived silica nanoparticles and composites for biosensors, bioimaging, drug delivery and supercapacitors: a review. *Environ Chem Lett*. <https://doi.org/10.1007/s10311-020-01123-5>
- Soylu H, Lambrecht FY, Ersöz O (2015) Gamma radiation shielding efficiency of a new lead-free composite material. *J Radioanal Nucl Chem* 305(2):529–534
- Srinivasan K, Samuel E (2017) Evaluation of radiation shielding properties of the polyvinyl alcohol/iron oxide polymer composite. *Med Phys* 42(4):273–278. [https://doi.org/10.4103/jmp.jmp\\_54\\_17](https://doi.org/10.4103/jmp.jmp_54_17)
- Surendhiran D, Sirajunnisa A, Tamilselvan K (2017) Silver-magnetic nanocomposites for water purification. *Environ Chem Lett* 15(3):367–386. <https://doi.org/10.1007/s10311-017-0635-1>
- Suteau C, Chiron M (2005) An iterative method for calculating gamma-ray build-up factors in multi-layer shields. *Radiat Prot Dosimetry* 116(1–4 Pt 2):489–492. <https://doi.org/10.1093/rpd/nci192>
- Taylor JJ (1954) Application of gamma ray build-up data to shield design, Westinghouse Electric, Corporation Atomic Power, Division U. S. Atomic Energy Commission, Bettis Atomic Power, Laboratory
- Tekin HO, Issa S (2018) Gamma radiation shielding properties of the hematite-serpentine concrete blended with WO<sub>3</sub> and Bi<sub>2</sub>O<sub>3</sub> micro and nano particles using MCNPX code. *Radiat Phys Chem*. <https://doi.org/10.1016/j.radphyschem.2018.05.002>
- Thuyavan YL, Anantharaman N, Arthanareeswaran G, Ismail AF, Mangalaraja RV (2015) Preparation and characterization of TiO<sub>2</sub>-sulfonated polymer embedded polyetherimide membranes for effective desalination application. *Desalination* 365:355–364. <https://doi.org/10.1016/j.desal.2015.03.004>
- Tian X, Liu T, Qingrui W, Abliz D, Ziegmann G (2016) Recycling and remanufacturing of 3D printed continuous carbon fiber reinforced PLA composites. *J Clean Prod*. <https://doi.org/10.1016/j.jclepro.2016.11.139>
- Tofa T, Laxman K, Paul S, Dutta J (2019) Visible light photocatalytic degradation of microplastic residues with zinc oxide nanorods. *Environ Chem Lett* 17:1341–1346. <https://doi.org/10.1007/s10311-019-00859-z>
- Tsepelev A, Kiseleva T, Zholudev S, Ковалева С, Grigoryeva T, Ivanenko I, Devyatkina E, Ilyushin A, Lyakhov N (2019) Electron irradiation resistance of the composite material structure based on ultra-high molecular polyethylene and boron carbide. *J Phys Conf Ser* 1347:012028. <https://doi.org/10.1088/1742-6596/1347/1/012028>
- Turner TA, Pickering SJ, Warrior NA (2011) Development of recycled carbon fibre moulding compounds—preparation of waste composites. *Compos B Eng* 42(3):517–525. <https://doi.org/10.1016/j.compositesb.2010.11.010>
- Vahabi SM, Shamsaie Zafarghandi M (2020) Build-up factors for water and soft tissue by MCNP using a co-centric multilayer model: comparative study. *J Instrum* 15:P05018. <https://doi.org/10.1088/1748-0221/15/05/p05018>
- Vahabi SM, Bahreinipour M, Shamsaie Zafarghandi M (2017) Determining the mass attenuation coefficients for some polymers using MCNP code: a comparison study. *Vacuum* 136:73–76. <https://doi.org/10.1016/j.vacuum.2016.11.011>
- Vilkov F, Lozovan A, Bazhanov A, Kasitsyn A, Schekoturova O, Solovov M (2017) Investigation of the radiation-protective properties of a highly filled liquid glass material. *J Surf Investig X-ray Synchrotron Neutron Tech* 11(5):912–916
- Wady P, Wasilewski A, Brock L, Edge R, Baidak A, McBride C, Leay L, Griffiths A, Vallés C (2019) Effect of ionising radiation on the mechanical and structural properties of 3D printed plastics. *Addit Manuf* 31:100907. <https://doi.org/10.1016/j.addma.2019.100907>
- Wang H, Zhang H, Su Y, Liu T, Yu H, Yang Y, Li X, Guo B (2015) Preparation and radiation shielding properties of Gd<sub>2</sub>O<sub>3</sub>/PEEK composites. *Polym Compos* 36(4):651–659
- Wen Y, Yuan J, Ma X, Wang S, Liu Y (2019) Polymeric nanocomposite membranes for water treatment: a review. *Environ Chem Lett*. <https://doi.org/10.1007/s10311-019-00895-9>
- Woodhead DJJ (2002) Protection of the environment from the effects of ionising radiation. *J Radiol Prot* 22(3):231
- Wozniak AI, Ivanov VS, Zhdanovich OA, Nazarov VI, Yegorov AS (2017) Modern approaches to polymer materials protecting from ionizing radiation. *Orient J Chem* 33(5):2148–2163
- Wu Y, Cao Y, Wu Y, Li DJM (2020) Mechanical properties and gamma-ray shielding performance of 3D-printed poly-ether-ether-ketone/tungsten composites. *Materials* 13(20):4475
- Yildirim Y, Oral A (2018) Structural changes in Poly(lactic acid)-zeolite nanocomposites exposed to 60 Co gamma rays. *Radiat Eff Defects Solids* 173:1–11. <https://doi.org/10.1080/10420150.2018.1462367>
- Yılmaz E, Baltas H, Kiris E, Ustabas İ, Cevik U, El-Khayatt A (2011) Gamma ray and neutron shielding properties of some concrete materials. *Ann Nucl Energy* 38(10):2204–2212
- Yurt Lambrecht F, Ersoz OA, Soylu HM (2016) Tungsten-ethylene vinyl acetate (EVA) composite as a gamma rays shielding material. *Indian J Pure Appl Phys* 54(12):793–796
- Zadegan S, Hosainipour M, Rezaie H, Ghassai H, Shokrgozar M (2011) Synthesis and biocompatibility evaluation of cellulose/hydroxyapatite nanocomposite scaffold in 1-n-allyl-3-methylimidazolium chloride. *Mater Sci Eng C* 31:954–961. <https://doi.org/10.1016/j.msec.2011.02.021>

- Zeng Q, Wang D, Yu A, Lu G (2002) Synthesis of polymer–montmorillonite nanocomposites by in situ intercalative polymerization. *Nanotechnology* 13(5):549
- Zein AA, Fel'dman VI, Egorov AV, Shmakova NA (2004) Effect of crystallinity degree on formation of radical ions in irradiated isotactic polystyrene. *Dokl Chem* 394(5):631–635
- Zhong W, Sui G, Jana S, Miller J (2009) Cosmic radiation shielding tests for UHMWPE fiber/nano-epoxy composites. *Compos Sci Technol* 69:2093–2097. <https://doi.org/10.1016/j.compscitech.2008.10.004>
- Zhou K, Gong K, Zhou Q, Zhao S, Guo H, Qian X (2020) Estimating the feasibility of using industrial solid wastes as raw material for polyurethane composites with low fire hazards. *J Clean Prod* 257:120606. <https://doi.org/10.1016/j.jclepro.2020.120606>
- Zulkiffi NI, Samat N, Anuar H, Zainuddin N (2015) Mechanical properties and failure modes of recycled polypropylene/microcrystalline cellulose composites. *Mater Des* 69:114–123

**Publisher's Note** Springer Nature remains neutral with regard to jurisdictional claims in published maps and institutional affiliations.